Episodic Multi-Task Learning with Heterogeneous Neural Processes

Jiayi Shen[1], **Xiantong Zhen**[1,2] *, **Qi (Cheems) Wang**[3], **Marcel Worring**[1]

[1]University of Amsterdam, Netherlands, {j.shen, m.worring}@uva.nl

[2] Inception Institute of Artificial Intelligence, Abu Dhabi, UAE, zhenxt@gmail.com

[3] Kaiyuan Mathematical Sciences Institute, Changsha, China, hhq123go@gmail.com

Abstract

This paper focuses on the data-insufficiency problem in multi-task learning within an episodic training setup. Specifically, we explore the potential of heterogeneous information across tasks and meta-knowledge among episodes to effectively tackle each task with limited data. Existing meta-learning methods often fail to take advantage of crucial heterogeneous information in a single episode, while multi-task learning models neglect reusing experience from earlier episodes. To address the problem of insufficient data, we develop Heterogeneous Neural Processes (HNPs) for the episodic multi-task setup. Within the framework of hierarchical Bayes, HNPs effectively capitalize on prior experiences as meta-knowledge and capture task-relatedness among heterogeneous tasks, mitigating data-insufficiency. Meanwhile, transformer-structured inference modules are designed to enable efficient inferences toward meta-knowledge and task-relatedness. In this way, HNPs can learn more powerful functional priors for adapting to novel heterogeneous tasks in each meta-test episode. Experimental results show the superior performance of the proposed HNPs over typical baselines, and ablation studies verify the effectiveness of the designed inference modules.

1 Introduction

Deep learning models have made remarkable progress with the help of the exponential increase in the amount of available training data [1]. However, many practical scenarios only have access to limited labeled data [2]. Such data-insufficiency sharply degrades the model's performance [2, 3]. Both meta-learning and multi-task learning have the potential to alleviate the data-insufficiency issue. Meta-learning can extract meta-knowledge from past episodes and thus enables rapid adaptation to new episodes with a few examples only [4–7]. Meanwhile, multi-task learning exploits the correlation among several tasks and results in more accurate learners for all tasks simultaneously [8–11]. However, the integration of meta-learning and multi-task learning in overcoming the data-insufficiency problem is rarely investigated.

In episodic training [4], existing meta-learning methods [4–7, 12, 13] in every meta-training or meta-test episode learn a single-task. In this paper, we refer to this conventional setting as *episodic single-task learning*. This setting restricts the potential for these models to explore task-relatedness within each episode, leaving the learning of multiple heterogeneous tasks in a single episode under-explored. We consider multiple tasks in each episode as *episodic multi-task learning*. The crux of episodic multi-task learning is to generalize the ability of exploring task-relatedness from meta-training to meta-test episodes. The differences between episodic single-task learning and episodic multi-task learning are illustrated in Figure 1. To be specific, we restrict the scope of the problem

---

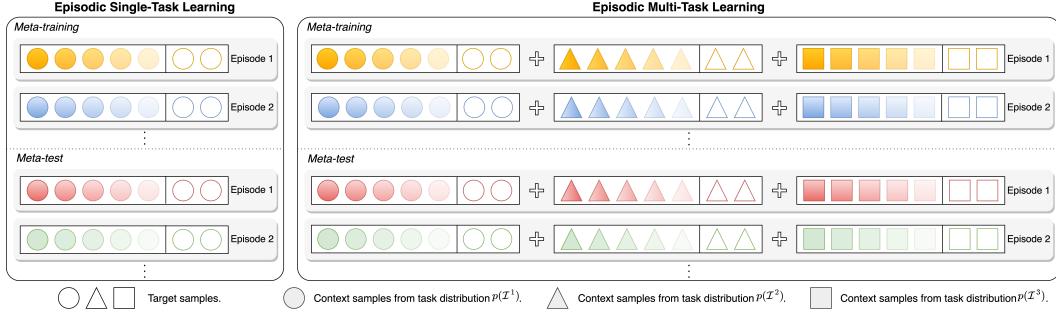*Currently with United Imaging Healthcare, Co., Ltd., China.

Figure 1: **Illustration of episodic multi-task learning.** Each row corresponds to a meta-training or meta-test episode. Different colors represent different label spaces among episodes; the same color with different shades represents different categories in the same task. Compared with episodic single-task learning, episodic multi-task learning simultaneously handles several related tasks in a single episode.

setup to the case where tasks in each meta-training or meta-test episode are heterogeneous but also relate to each other by sharing the same target space.

The neural process (NP) family [12, 13], as typical meta-learning probabilistic models [14], efficiently quantifies predictive uncertainty with limited data, making it in principle well-suited for tackling the problem of data-insufficiency. However, in practice, it is challenging for vanilla NPs [12] with a global latent variable to encode beneficial heterogeneous information in each episode. This issue is also known as the expressiveness bottleneck [15, 16], which weakens the model's capacity to handle insufficient data, especially when faced with diverse heterogeneous tasks.

To better resolve the data-insufficiency problem, we develop Heterogeneous Neural Processes (HNPs) for episodic multi-task learning. As a new member of the NP family, HNPs improve the expressiveness of vanilla NPs by introducing a hierarchical functional space with global and local latent variables. The remainder of this work is structured as follows: We introduce our method in Section (2). Related work is overviewed in Section (3). We report experimental results with analysis in Section (4), after which we conclude with a technical discussion, existing limitations, and future extensions. In detail, our technical contributions are two-fold:

- Built on the hierarchical Bayes framework, our developed HNPs can simultaneously generalize meta-knowledge from past episodes to new episodes and exploit task-relatedness across heterogeneous tasks in every single episode. This mechanism makes HNPs more powerful when encoding complex conditions into functional priors.

- We design transformer-structured inference modules to infer the hierarchical latent variables, capture task-relatedness, and learn a set of tokens as meta-knowledge. The designed modules can fuse the meta-knowledge and heterogeneous information from context samples in a unified manner, boosting the generalization capability of HNPs across tasks and episodes.

Experimental results show that the proposed HNPs together with transformer-structured inference modules, can exhibit superior performance on regression and classification tasks under the episodic multi-task setup.

2 Methodology

Notations [2]**.** We will now formally define episodic multi-task learning. For a single episode τ, we consider M heterogeneous but related tasks $\mathcal{I}_\tau^{1:M} = \{\mathcal{I}_\tau^m\}_{m=1}^M$. Notably, the subscript denotes an episode, while superscripts are used to distinguish tasks in this episode. In the episodic multi-task setup, tasks in a single episode are heterogeneous since they are sampled from different task distributions $\{p(\mathcal{I}^m)\}_{m=1}^M$, but are related at the same time as they share the target space $\mathcal{Y}_\tau$.

---

[2] For ease of presentation, we abbreviate a set $\{(\cdot)^m\}_{m=1}^M$ as $(\cdot)^{1:M}$, where M is a positive integer. Likewise, $\{(\cdot)_o\}_{o=1}^O$ is abbreviated as $(\cdot)_{1:O}$. For convenience, the notation table is provided in Appendix B.

To clearly relate to the modeling of vanilla neural processes [12], this paper follows its nomenclature to define each task. Note that in vanilla neural processes *context* and *target* are often respectively called *support* and *query* in conventional meta-learning [4, 5]. Each task $\mathcal{I}_\tau^m$ contains a context set with limited training data $\mathcal{C}_\tau^m = \{\bar{x}_{\tau,i}^m, \bar{y}_{\tau,i}^m\}_{i=1}^{N_\mathcal{C}}$ and a target set $\mathcal{T}_\tau^m = \{x_{\tau,j}^m, y_{\tau,j}^m\}_{j=1}^{N_\mathcal{T}}$, where $N_\mathcal{C}$ and $N_\mathcal{T}$ are the numbers of context samples and target samples, respectively. $\bar{x}_{\tau,i}^m$ and $x_{\tau,j}^m$ represent features of context and target samples; while $\bar{y}_{\tau,i}^m, y_{\tau,j}^m \in \mathcal{Y}_\tau$ are their corresponding targets, where $i = 1, 2, ..., N_\mathcal{C}; j = 1, 2, .., N_\mathcal{T}; m = 1, 2, ..., M$. For simplicity, we denote the set of target samples and their corresponding ground-truths by $\mathbf{x}_\tau^m = \{x_{\tau,j}^m\}_{j=1}^{N_\mathcal{T}}, \mathbf{y}_\tau^m = \{y_{\tau,j}^m\}_{j=1}^{N_\mathcal{T}}$. For an episode τ, episodic multi-task learning aims to perform simultaneously well on each corresponding target set $\mathcal{T}_\tau^m, m = 1, 2.., M$, given the collection of context sets $\mathcal{C}_\tau^{1:M}$.

For classification, this paper follows the protocol of meta models [4, 5, 17], such as O-way K-shot setup, clearly suffering from the data-insufficiency problem. Thus, episodic multi-task classification can be cast as a M-task O-way K-shot supervised learning problem. An episode has M related classification tasks, and each of them has a context set with K different instances from each of the O classes [5]. It is worth mentioning that the target spaces of meta-training episodes do not overlap with any categories in those of meta-test episodes.

2.1 Modeling and Inference of Heterogeneous Neural Processes

We now present the proposed heterogeneous neural process. The proposed model inherits the advantages of multi-task learning and meta-learning, which can exploit task-relatedness among heterogeneous tasks and extract meta-knowledge from previous episodes. Next, we characterize the generative process, clarify the modeling within the hierarchical Bayes framework, and derive the approximate evidence lower bound (ELBO) in optimization.

Generative Processes. To get to our proposed method HNPs, we extend the distribution over a single function $p(f_\tau)$ as used in vanilla NPs to a joint distribution of multiple functions $p(f_\tau^{1:M})$ for all heterogeneous tasks in a single episode τ. In detail, the underlying multi-task function distribution $p(f_\tau^{1:M})$ is inferred from a collection of context sets $\mathcal{C}_\tau^{1:M}$ and learnable meta-knowledge $\omega, \nu^{1:M}$. Note that ω represents the shared meta-knowledge for all tasks, and ν^m denotes the task-specific meta-knowledge corresponding to the task distribution $p(\mathcal{I}^m)$. Hence, we can formulate the predictive distribution for every single episode as follows:

$$p(\mathcal{T}_\tau^{1:M}|\mathcal{C}_\tau^{1:M}; \omega, \nu^{1:M}) = \int p(\mathbf{y}_\tau^{1:M}|\mathbf{x}_\tau^{1:M}, f_\tau^{1:M}) p(f_\tau^{1:M}|\mathcal{C}_\tau^{1:M}; \omega, \nu^{1:M}) df_\tau^{1:M}, \quad (1)$$

where $p(f_\tau^{1:M}|\mathcal{C}_\tau^{1:M}; \omega, \nu^m)$ denotes the data-dependent functional prior for multiple tasks of the episode τ. The functional prior encodes context sets from all heterogeneous tasks and quantifies uncertainty in the functional space. Nevertheless, it is less optimal to characterize multi-task function generative processes with vanilla NPs, since the single latent variable limits the capacity of the latent space to specify the complicated functional priors. This expressiveness bottleneck in vanilla NPs is particularly severe for our episodic multi-task learning since each episode has diverse heterogeneous tasks with insufficient data.

Modeling within the Hierarchical Bayes Framework. To mitigate the expressiveness bottleneck of vanilla NPs, we model HNPs by parameterizing each task-specific function within a hierarchical Bayes framework. As illustrated in Figure 2, HNPs integrate a global latent representation $\mathbf{z}_\tau^m$ and a set of local latent parameters $\mathbf{w}_{\tau,1:O}^m$ to model each task-specific function f_τ^m. Specifically, the latent variables are introduced at different levels: $\mathbf{z}_\tau^m$ encodes task-specific context information from $\mathcal{C}_\tau^m$ and ν^m in the representation level. $\mathbf{w}_{\tau,1:O}^m$ encode prediction-aware information for a task-specific decoder from $\mathcal{C}_\tau^{1:M}$ and ω in the parameter level, where O is the dimension of the decoder. For example, the dimension is the size of the target space when performing classification tasks.
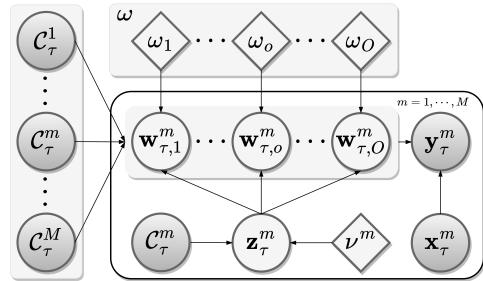

Figure 2: **Graphical model of the proposed HNPs in a single episode.** Filled shapes indicate observations. Probabilistic and deterministic variables are indicated by unfilled circles and diamonds, respectively.

3

Notably, each local latent parameter is conditioned on the global latent representation, which controls access to all context sets in the episode for the corresponding task. Our method differs from previous hierarchical architectures [16, 18–20] in the NP family since the local latent parameters of our HNPs are prediction-aware and explicitly constitute a decoder for the subsequent inference processes.

In practice, we assume that distributions of each task-specific function are conditionally independent. Thus, with the introduced hierarchical latent variables for each task in the episode, we can factorize the prior distribution over multiple functions in Eq. (1) into:

$$p(f_\tau^{1:M}|\mathcal{C}_\tau^{1:M};\omega,\nu^{1:M}) = \prod_{m=1}^{M} p(\mathbf{z}_\tau^m|\mathcal{C}_\tau^m;\nu^m)p(\mathbf{w}_{\tau,1:O}^m|\mathbf{z}_\tau^m,\mathcal{C}_\tau^{1:M};\omega), \tag{2}$$

where $p(\mathbf{z}_\tau^m|\mathcal{C}_\tau^m;\nu^m)$ and $p(\mathbf{w}_{\tau,1:O}^m|\mathbf{z}_\tau^m,\mathcal{C}_\tau^{1:M};\omega)$ are prior distributions of the global latent representation and the local latent parameters to induce the task-specific function distribution.

By integrating Eq. (2) into Eq. (1), we rewrite the modeling of HNPs in the following form:

$$p(\mathcal{T}_\tau^{1:M}|\mathcal{C}_\tau^{1:M};\omega,\nu^{1:M}) = \prod_{m=1}^{M} \int \Big\{ \int p(\mathbf{y}_\tau^m|\mathbf{x}_\tau^m,\mathbf{w}_{\tau,1:O}^m)$$
$$p(\mathbf{w}_{\tau,1:O}^m|\mathbf{z}_\tau^m,\mathcal{C}_\tau^{1:M};\omega)d\mathbf{w}_{\tau,1:O}^m \Big\}p(\mathbf{z}_\tau^m|\mathcal{C}_\tau^m;\nu^m)d\mathbf{z}_\tau^m, \tag{3}$$

where $p(\mathbf{y}_\tau^m|\mathbf{x}_\tau^m,\mathbf{w}_{\tau,1:O}^m)$ is the function distribution for the task $\mathcal{I}_\tau^m$ in HNPs. This distribution is obtained by the matrix multiplication of $\mathbf{x}_\tau^m$ and all local latent parameters $\mathbf{w}_{\tau,1:O}^m$.

Compared with most NP models [12, 16, 18, 19] employing only latent representations, HNPs infer both latent representations and parameters in the hierarchical architecture from multiple heterogeneous context sets and learnable meta-knowledge. Our model specifies a richer and more intricate functional space by leveraging the hierarchical uncertainty inherent in the context sets and meta-knowledge. This theoretically yields more powerful functional priors to induce multi-task function distributions.

Moreover, we claim that the developed model constitutes an *exchangeable stochastic process* and demonstrate this via Kolmogorov Extension Theorem [21]. Please refer to Appendix B for the proof.

Approximate ELBO. Since both exact functional posteriors and priors are intractable, we apply variational inference to the proposed HNPs in Eq. (3). This results in the approximate ELBO:

$$L_{\text{HNPs}}(\omega,\nu^{1:M},\theta,\phi) = \sum_{m=1}^{M} \Big\{ \mathbb{E}_{q_\theta(\mathbf{z}_\tau^m|\mathcal{T}_\tau^m;\nu^m)}\Big\{ \mathbb{E}_{q_\phi(\mathbf{w}_{\tau,1:O}^m|\mathbf{z}_\tau^m,\mathcal{T}_\tau^{1:M};\omega)}[\log p(\mathbf{y}_\tau^m|\mathbf{x}_\tau^m,\mathbf{w}_{\tau,1:O}^m)]$$

$$- \mathbb{D}_{\text{KL}}[q_\phi(\mathbf{w}_{\tau,1:O}^m|\mathbf{z}_\tau^m,\mathcal{T}_\tau^{1:M};\omega)||p_\phi(\mathbf{w}_{\tau,1:O}^m|\mathbf{z}_\tau^m,\mathcal{C}_\tau^{1:M};\omega)]\Big\} - \mathbb{D}_{\text{KL}}[q_\theta(\mathbf{z}_\tau^m|\mathcal{T}_\tau^m;\nu^m)||p_\theta(\mathbf{z}_\tau^m|\mathcal{C}_\tau^m;\nu^m)]\Big\},$$
$$\tag{4}$$

where $q_\theta(\mathbf{z}_\tau^m|\mathcal{T}_\tau^m;\nu^m)$ and $q_\phi(\mathbf{w}_{\tau,1:O}^m|\mathbf{z}_\tau^m,\mathcal{T}_\tau^{1:M};\omega)$ are variational posteriors of their corresponding latent variables. θ and ϕ are parameters of inference modules for $\mathbf{z}_\tau^m$ and $\mathbf{w}_{\tau,1:O}^m$, respectively. Following the protocol of vanilla NPs [12], the priors use the same inference modules as variational posteriors for tractable optimization. In this way, the KL-divergence terms in Eq. (4) encourage all latent variables inferred from the context sets to stay close to those inferred from the target sets, enabling effective function generation with few examples. Details on the derivation of the approximate ELBO and its tractable optimization are attached in Appendix C.

2.2 Transformer-Structured Inference Module

In order to infer the prior and variational posterior distributions in Eq. (4), it is essential to develop well-designed approximate inference modules. This is non-trivial and closely related to the performance of HNPs. Here we adopt a transformer structure as the inference module to better exploit task-relatedness from the meta-knowledge and the context sets in the episode. More specifically, the previously mentioned meta-knowledge $\omega = \omega_{1:O}$ and $\nu^{1:M}$ are instantiated as learnable tokens to induce the distributions of hierarchical latent variables in the proposed model.

Without loss of generality, in the next, we provide an example of transformer-structured inference modules for prior distributions in classification scenarios. Details of the inference modules in regression scenarios can be found in Appendix D. In Figure 3, a diagram of the transformer-structured
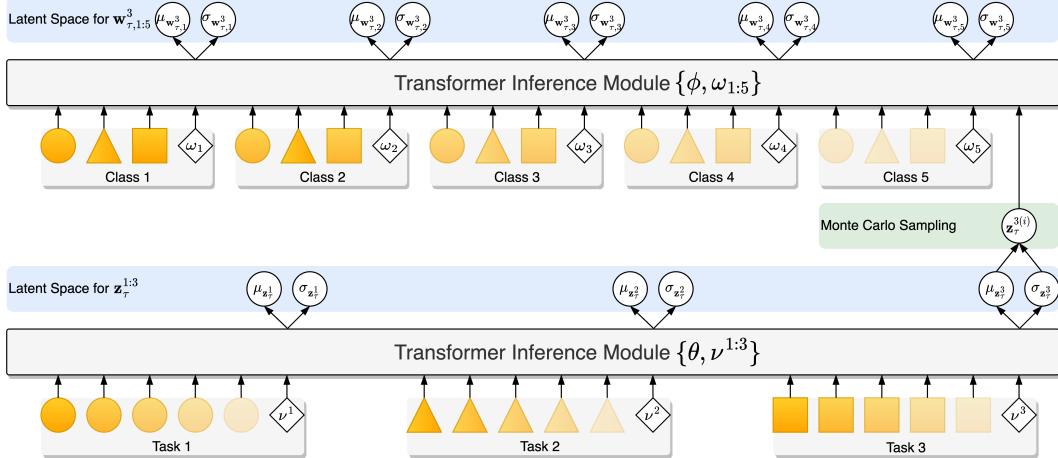
Figure 3: **A diagram of transformer-structured inference modules of HNPs for the first meta-training episode in Figure 1 under the `3-task 5-way 1-shot` setting.** For clarity, we display the inference process of the local latent parameters specific to the third task in the episode.

inference modules is displayed under the `3-task 5-way 1-shot` setting. In this case, the number of context samples is the same as the size of the target space, and thus we have $\mathcal{C}_\tau^m = \{\bar{x}_{\tau,o}^m, \bar{y}_{\tau,o}^m\}_{o=1}^O$, where O is set as 5. In episodic training, labels in context sets are always available during inference.

Transformer-Structured Inference Module $\{\theta, \nu^m\}$ for $\mathbf{z}_\tau^m$. In the proposed HNPs, each global latent representation encodes task-specific information relevant to the considered task in the episode as $p_\theta(\mathbf{z}_\tau^m|\mathcal{C}_\tau^m; \nu^m)$. The learnable token ν^m preserves the meta-knowledge from previous episodes for specific tasks, which are sampled from the corresponding task distribution $p(\mathcal{I}^m)$. The role of ν^m is to help the model adapt efficiently to such specific tasks in meta-test episodes.

In detail, we set the dimension of the learnable token ν^m to the same as that of the features $\bar{x}_{\tau,1:O}^m$. Then the transformer-structured inference module θ fuses them in a unified manner by taking $[\bar{x}_{\tau,1:O}^m; \nu^m]$ as the input. The module θ outputs the mean and variance of the corresponding prior distribution. The inference steps for the global latent representation $\mathbf{z}_\tau^m$ are:

$$[\widetilde{x}_{\tau,1:O}^m; \widetilde{\nu}^m] = \texttt{MSA}(\texttt{LN}([\bar{x}_{\tau,1:O}^m; \nu^m])) + [\bar{x}_{\tau,1:O}^m; \nu^m], \tag{5}$$

$$[\widehat{x}_{\tau,1:O}^m; \widehat{\nu}^m] = \texttt{MLP}(\texttt{LN}([\widetilde{x}_{\tau,1:O}^m; \widetilde{\nu}^m])) + [\widetilde{x}_{\tau,1:O}^m; \widetilde{\nu}^m], \tag{6}$$

$$p_\theta(\mathbf{z}_\tau^m|\mathcal{C}_\tau^m; \nu^m) = \mathcal{N}(\mathbf{z}_\tau^m; \mu_{\mathbf{z}_\tau^m}, \sigma_{\mathbf{z}_\tau^m}), \tag{7}$$

where $\mu_{\mathbf{z}_\tau^m} = \texttt{MLP}(\widehat{\nu}^m)$, $\sigma_{\mathbf{z}_\tau^m} = \texttt{Softplus}(\texttt{MLP}(\widehat{\nu}^m))$. The transformer-structured inference module includes a multi-headed self-attention (`MSA`) and three multi-layer perceptrons (`MLP`). The layer normalization (`LN`) is "pre-norm" as done in [22]. `Softplus` is the activation function to output the appropriate value as the variance of the prior distribution [23].

Transformer-Structured Inference Module $\{\phi, \omega_{1:O}\}$ for $\mathbf{w}_{\tau,1:O}^m$. Likewise, each learnable token ω_o corresponds to a local latent parameter $\mathbf{w}_{\tau,o}^m$. With the learnable tokens $\omega_{1:O}$, we reformulate the prior distribution of local latent parameters as $p_\phi(\mathbf{w}_{\tau,1:O}^m|\mathbf{z}_\tau^m, \mathcal{C}_\tau^{1:M}; \omega_{1:O})$. In this way, we learn the shared knowledge, inductive biases across all tasks, and their distribution at a parameter level, which in practical settings can capture epistemic uncertainty.

To be specific, the prior distribution can be factorized as $\prod_{o=1}^O p_\phi(\mathbf{w}_{\tau,o}^m|\mathbf{z}_\tau^m, \mathcal{C}_\tau^{1:M}; \omega_o)$, where all local latent parameters are assumed to be conditionally independent. For each local latent parameter $\mathbf{w}_{\tau,o}^m$, the transformer-structured inference module ϕ takes $[\bar{x}_{\tau,o}^{1:M}, \omega_o]$ as input and outputs the corresponding prior distribution, where $\bar{x}_{\tau,o}^{1:M}$ are deep features from the same class o in the episode and ω_o is the corresponding learnable token. Here the inference steps for $\mathbf{w}_{\tau,o}^m$ are as follows:

$$[\widetilde{x}_{\tau,o}^{1:M}; \widetilde{\omega}_o] = \texttt{MSA}(\texttt{LN}([\bar{x}_{\tau,o}^{1:M}; \omega_o])) + [\bar{x}_{\tau,o}^{1:M}; \omega_o], \tag{8}$$

5

$$[\widehat{x}_{\tau,o}^{1:M}; \widehat{\omega}_o] = \texttt{MLP}(\texttt{LN}([\widetilde{x}_{\tau,o}^{1:M}; \widetilde{\omega}_o])) + [\widetilde{x}_{\tau,o}^{1:M}; \widetilde{\omega}_o], \tag{9}$$

$$p_\phi(\mathbf{w}_{\tau,o}^m | \mathbf{z}_\tau^m, \mathcal{C}_\tau^{1:M}; \omega_o) = \mathcal{N}(\mathbf{w}_{\tau,o}^m; \mu_{\mathbf{w}_{\tau,o}^m}, \sigma_{\mathbf{w}_{\tau,o}^m}), \tag{10}$$

where $\mu_{\mathbf{w}_{\tau,o}^m} = \texttt{MLP}(\widehat{\omega}_o, \mathbf{z}_\tau^{m(i)}), \sigma_{\mathbf{w}_{\tau,o}^m} = \texttt{Softplus}(\texttt{MLP}(\widehat{\omega}_o, \mathbf{z}_\tau^{m(i)}))$. $\mathbf{z}_\tau^{m(i)}$ is a Monte Carlo sample from the variational posterior of the corresponding global latent representation during meta-training.

Both transformer-structured inference modules use the refined tokens $\widehat{\nu}^m$ and $\widehat{\omega}_o$ to obtain a global latent representation and a local latent parameter, respectively. The introduced tokens preserve the specific meta-knowledge for each latent variable during inference. Compared with the θ-parameterised inference module exploring the intra-task relationships, the ϕ-parameterised inference module enables the exploitation of the inter-task relationships to reason over each local latent parameter. Thus, the introduced tokens can be refined with relevant information from the heterogeneous context sets. By integrating meta-knowledge and heterogeneous context sets, HNPs can reduce the negative transfer of task-specific knowledge among heterogeneous tasks in each episode. Please refer to Appendix E for algorithms.

3   Related Work

Multi-Task Learning.   Multi-task learning can operate in various settings [9]. Here we roughly separate the settings of MTL into two branches: (1) Single-input multi-output (SIMO) [24–30], where tasks are defined by different supervision information for the same input. (2) Multi-input multi-output (MIMO) [11, 10, 31–34], where heterogeneous tasks follow different data distributions. This work considers the MIMO setup of multi-task learning with episodic training.

In terms of modeling methods, from a processing perspective, existing MTL methods can be roughly categorized into two groups: (1) Probabilistic MTL methods [11, 19, 35–41], which employ the Bayes framework to characterize probabilistic dependencies among tasks. (2) Deep MTL models [10, 32, 24–26, 42–48], which directly utilize deep neural networks to discover information-sharing mechanisms across tasks. However, deep MTL models rely on large amounts of training data and tend to overfit when encountering the data-insufficiency problem. Meanwhile, previous probabilistic MTL methods consider a small number of tasks that occur at the same time, limiting their applicability in real-world systems.

Meta-Learning.   Meta-learning aims to find strategies to quickly adapt to unseen tasks with a few examples [49, 4, 5, 50]. There exist a couple of branches in meta-learning methods, such as metrics-based methods [6, 51–57] and optimization-based methods [5, 58–68]. Our paper focuses on a probabilistic meta-learning method, namely neural processes, that can quantify predictive uncertainty. Models in this family [7, 12, 13, 15, 16, 18, 69–73] can approximate stochastic processes in neural networks. Vanilla NPs [12] usually encounter the expressiveness bottleneck because their functional priors are not rich enough to generate complicated functions [15, 16]. [7] introduces deterministic variables to model predictive distributions for meta-learning scenarios directly. Most NP-based methods only focus on a single task during inference [7, 12, 15, 16, 14], which leaves task-relatedness between heterogeneous tasks in a single episode an open problem.

This paper combines multi-task learning and meta-learning paradigms to tackle the data-insufficiency problem. Our work shares the high-level goal of exploiting task-relatedness in an episode with [19, 74, 75]. Concerning the multi-task scenarios, the main differences are: [19, 74, 75] handles multiple attributes and multi-sensor data under the SIMO setting, while our work performs for the MIMO setting where tasks are heterogeneous and distribution shifts exist. Moreover, [76] theoretically addresses the conclusion that MTL methods are powerful and efficient alternatives to gradient-based meta-learning algorithms. However, our method inherits the advantages of multi-task learning and meta-learning: simultaneously generalizing meta-knowledge from past to new episodes and exploiting task-relatedness across heterogeneous tasks in every single episode. Thus, our method is more suitable for solving the data-insufficiency problem. Intuitive comparisons with related paradigms such as *cross-domain few-shot learning* [77–82], *multimodal meta-learning* [83–87, 56] and *cross-modality few-shot learning* [88–90] are provided in Appendix A.

4 Experiments

We evaluate the proposed HNPs and baselines on three benchmark datasets under the episodic multi-task setup. Sec. 4.1 and Sec. 4.2 provide experimental results for regression and classification, respectively. Ablation studies are in Sec. 4.3. More comparisons with recent works on extra datasets are provided in Appendix F. Additional results under the convectional MIMO setup without episodic training can be found in Appendix G & H.

4.1 Episodic Multi-Task Regression

Dataset and Settings. To evaluate the benefit of HNPs over typical NP baselines in uncertainty quantification, we conduct experiments in several 1D regression tasks. The baselines include conditional neural processes (CNPs [13]), vanilla neural processes (NPs [12]), and attentive neural processes (ANPs [15]). As a toy example, we construct multiple tasks with different task distributions: each task's input set is defined on separate intervals without overlap.

Given four different tasks in an episode, their input sets are $\mathbf{x}_\tau^{1:4}$. Each input set contains a few instances, drawn uniformly at random from separate intervals, such as $\mathbf{x}_\tau^1 \in [-4, -2)$, $\mathbf{x}_\tau^2 \in [-2, 0)$, $\mathbf{x}_\tau^3 \in [0, 2)$, and $\mathbf{x}_\tau^4 \in [2, 4)$. All tasks in an episode are related by sharing the same ground truth function. Following [12, 18], function-fitting tasks are generated with Gaussian processes (GPs). Here a zero mean Gaussian process $y^{(0)} \sim \mathcal{GP}(0, k(\cdot, \cdot))$ is used to produce $\mathbf{y}_\tau^{1:4}$ for the inputs from all tasks $\mathbf{x}_\tau^{1:4}$. A radial basis kernel $k(x, x') = \sigma^2 \exp(-(x - x')^2)/2l^2)$, with $l = 0.4$ and $\sigma = 1.0$ is used.

Figure 4: **Performance comparisons on the episodic multi-task** 1**-D function regression using** 5 **context points (black dots) for each task.** Black curves are ground truth, and blue ones are predicted results. The shadow regions are ± 3 standard derivations from the mean [18].

Results and Discussions. As shown in Figure 4, CNPs, ANPs, and our HNPs exhibit more reasonable uncertainty than NPs in Figure 4: lower variances are predicted around observed (context) points with higher variances around unobserved points. Furthermore, NPs and ANPs detrimentally impact the smoothness of the predicted curves, whereas HNPs yield smoother predictive curves with reliable uncertainty estimation. These observations suggest that integrating correlation information across related tasks and meta-knowledge in HNPs can improve uncertainty quantification in multi-task regression.

To quantify uncertainty we use the average negative log-likelihood (the lower, the better). As shown in Table 1, our HNPs achieve a lower average negative log-likelihood than baselines, demonstrating our method's effectiveness in uncertainty estimation.

Table 1: **Average negative log-likelihoods over target points from all tasks.**

Methods	CNPs	NPs	ANPs	HNPs
Avg. NLL	0.0935	0.8649	-0.1165	-0.5207

4.2 Episodic Multi-task Classification

Datasets and Settings. We use Office-Home [91] and DomainNet [92] as episodic multi-task classification datasets. Office-Home contains images from four domains: Artistic (A), Clipart (C), Product (P) and Real-world (R). Each domain contains images from 65 categories collected from office and home environments. Note that all domains share the whole target space. The numbers of meta-training classes and meta-test classes are 40 and 25, respectively. There are about 15, 500 images in total. DomainNet has six distinct domains: Clipart, Infograph, Painting, Quickdraw, Real and Sketch. It includes approximately 0.6 million images distributed over 345 categories. The
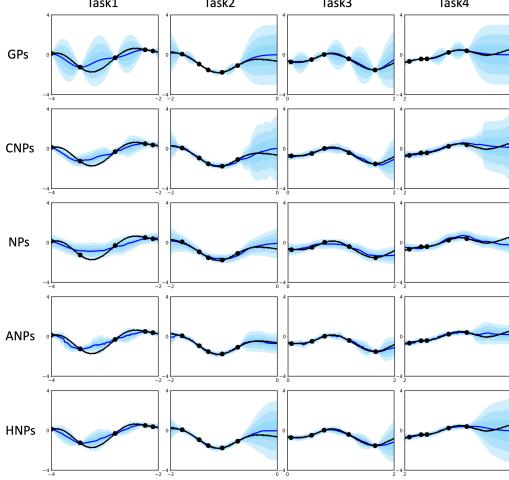
Table 2: **Comparative results (95% confidence interval) for episodic multi-task classification on** `Office-Home` **and** `DomainNet`**.** Best results are indicated in bold.

| | Office-Home | | | | DomainNet | | | |
| | 4-task 5-way | | 4-task 20-way | | 6-task 5-way | | 6-task 20-way | |
Method	1-shot	5-shot	1-shot	5-shot	1-shot	5-shot	1-shot	5-shot
ERM [93]	66.04 $\pm$0.61	73.62 $\pm$0.55	39.25 $\pm$0.24	47.14 $\pm$0.18	59.95 $\pm$0.52	68.52 $\pm$0.44	38.62 $\pm$0.22	47.85 $\pm$0.20
VMTL [11]	49.71 $\pm$0.48	65.75 $\pm$0.47	27.50 $\pm$0.14	42.82 $\pm$0.13	42.24 $\pm$0.39	57.37 $\pm$0.43	18.05 $\pm$0.11	31.38 $\pm$0.15
MAML [5]	60.58 $\pm$0.60	75.29 $\pm$0.53	34.29 $\pm$0.19	48.39 $\pm$0.20	53.21 $\pm$0.46	65.24 $\pm$0.47	17.10 $\pm$0.12	20.35 $\pm$0.14
Proto. Net. [6]	57.19 $\pm$0.53	74.97 $\pm$0.46	32.72 $\pm$0.18	49.75 $\pm$0.16	53.71 $\pm$0.48	68.80 $\pm$0.42	31.90 $\pm$0.19	47.59 $\pm$0.18
DGPs [94]	65.89 $\pm$0.53	79.96 $\pm$0.38	31.48 $\pm$0.18	49.46 $\pm$0.18	50.93 $\pm$0.42	63.32 $\pm$0.38	25.46 $\pm$0.15	38.63 $\pm$0.17
CNPs [13]	43.33 $\pm$0.56	55.07 $\pm$0.63	10.57 $\pm$0.10	12.02 $\pm$0.11	37.90 $\pm$0.45	40.53 $\pm$0.44	5.12 $\pm$0.10	5.14 $\pm$0.10
NPs [12]	33.66 $\pm$0.48	53.99 $\pm$0.60	5.25 $\pm$0.16	11.40 $\pm$0.11	20.58 $\pm$0.51	20.53 $\pm$0.53	5.12 $\pm$0.09	5.11 $\pm$0.09
TNP-D [95]	65.49 $\pm$0.53	78.94 $\pm$0.43	41.61 $\pm$0.22	59.19 $\pm$0.21	49.10 $\pm$0.42	67.39 $\pm$0.40	28.83 $\pm$0.17	47.69 $\pm$0.18
HNPs	**76.29** $\pm$0.51	**80.80** $\pm$0.42	**51.82** $\pm$0.23	**59.97** $\pm$0.18	**62.36** $\pm$0.53	**69.38** $\pm$0.42	**39.32** $\pm$0.23	**48.56** $\pm$0.19

numbers of meta-training classes and meta-test classes are 276 and 69, respectively. Here one domain corresponds to a specific task distribution in the episodic multi-task setting.

When it comes to the episodic multi-task classification, we compare HNPs with the following three branches: (1) *Multi-task learning methods*: ERM [93] directly expands the training set of the current task with samples of related tasks. VMTL [11] is one of the state-of-the-art under the MIMO setting of multi-task learning. (2) *Meta-learning methods*: MAML [5], Proto.Net [6] and DGPs [94] address each task separately with no mechanism to leverage task-relatedness in a single episode. (3) *Methods from the NP family*: CNPs [13] and NPs [12] are established methods in the NP family. TNP-D [95] is recent NP work in sequential decision-making for a single task in each episode.

Results and Discussions.   The experimental results for episodic multi-task classification on `Office-Home` and `DomainNet` are reported in Table 2. We use the average accuracy across all task distributions as the evaluation metric. It can be seen that HNPs consistently outperform all baseline methods, demonstrating the effectiveness of HNPs in handling each task with limited data under the episodic multi-task classification setup.

NPs and CNPs do not work well under all episodic multi-task classification cases. This can be attributed to their limited expressiveness of the global representation and the weak capability to extract discriminative information from multiple contexts. In contrast, HNPs explicitly abstract discriminative information for each task in the episode with the help of local latent parameters, enhancing the expressiveness of the functional prior.

We also find that HNPs significantly surpass other baselines on `1-shot` `Office-Home` and `DomainNet`, both under the `4/6-task 5-way` and `4/6-task 20-way` settings. This further implies that HNPs can circumvent the effect of the problem of data-insufficiency by simultaneously exploiting task-relatedness across heterogeneous tasks and meta-knowledge among episodes.

4.3   Ablation Studies

Influence of Hierarchical Latent Variables.   We first investigate the roles of the global latent representation $\mathbf{z}_\tau^m$ and the local latent parameters $\mathbf{w}_{\tau,1:O}^m$ by leaving out individual inference modules. These experiments are performed on `Office-home` under the `4-task 5-way 1-shot` setting. We report the detailed performance for tasks sampled from a single task distribution (A/C/P/R) and the average accuracy across all task distributions (Avg.) in Table 3. The variants without specific latent variables are included in the comparison by removing the corresponding inference modules.

As shown in Table 3, both $\mathbf{z}_\tau^m$ and $\mathbf{w}_{\tau,1:O}^m$ benefit overall performance. Our method with hierarchical latent variables performs 9.20% better than the variant without both latent variables, 3.00% better than the variant without $\mathbf{z}_\tau^m$, and 5.18% better than the variant without $\mathbf{w}_{\tau,1:O}^m$. This indicates that latent variables of HNPs complement each other in representing con-

Table 3: **Effectiveness of global latent representations** $\mathbf{z}_\tau^m$ **and local latent parameters** $\mathbf{w}_{\tau,1:O}^m$ **in the model.** ✓ and ✗ denote whether the variants of HNPs have the corresponding latent variable or not.

$\mathbf{z}_\tau^m$	$\mathbf{w}_{\tau,1:O}^m$	A	C	P	R	Avg.
✗	✗	62.64 $\pm$0.72	56.87 $\pm$0.71	75.18 $\pm$0.79	73.68 $\pm$0.77	67.09 $\pm$0.63
✗	✓	69.39 $\pm$0.60	63.10 $\pm$0.61	80.66 $\pm$0.67	79.99 $\pm$0.62	73.29 $\pm$0.51
✓	✗	67.02 $\pm$0.67	60.70 $\pm$0.69	78.26 $\pm$0.76	78.47 $\pm$0.72	71.11 $\pm$0.59
✓	✓	**73.31** $\pm$0.63	**64.92** $\pm$0.68	**83.38** $\pm$0.66	**83.54** $\pm$0.64	**76.29** $\pm$0.51

8

text sets from multiple tasks and meta-knowledge. The variant without $\mathbf{w}_{\tau,1:O}^{m}$ underperforms the variant without $\mathbf{z}_{\tau}^{m}$ by 2.18%, in terms of the average accuracy. This demonstrates that $\mathbf{z}_{\tau}^{m}$ suffers more from the expressiveness bottleneck than $\mathbf{w}_{\tau,1:O}^{m}$, weakening the models' discriminative ability. For classification, local latent parameters are more crucial than a global latent representation in revealing the discriminating knowledge from multiple heterogeneous context sets.

Influence of Transformer-Structured Inference Modules. To further understand our transformer-structured inference modules (Trans. w learnable tokens), we examine the performance against two other options: inference modules that solely utilize a multi-layer perceptron (MLP) and the variants that do not incorporate any learnable tokens (Trans. w/o learnable tokens). We also compare the probabilistic and deterministic versions of such inference modules. The deterministic variants consider the deterministic embedding for the hierarchical latent variables.

As shown in Table 4, our inference modules consistently outperform the variants, regardless of whether the inference network is probabilistic or deterministic. When using the probabilistic one, our inference modules respectively achieve 1.04% and 2.99% performance gains over Trans. w/o learnable tokens and MLP under the 4-task 5-way 1-shot setting. This implies the importance of learn-

Table 4: **Performance comparisons between our transformer inference modules (Trans. w learnable tokens) and other alternatives.**

	Inference networks	1-shot	5-shot
Deterministic	MLP	$64.93 _{\pm 0.66}$	$72.39 _{\pm 0.56}$
	Trans. w/o learnable tokens	$70.22 _{\pm 0.62}$	$76.15 _{\pm 0.54}$
	Trans. w learnable tokens	$70.61 _{\pm 0.56}$	$76.70 _{\pm 0.50}$
Probabilistic	MLP	$73.30 _{\pm 0.59}$	$77.94 _{\pm 0.48}$
	Trans. w/o learnable tokens	$75.25 _{\pm 0.55}$	$80.42 _{\pm 0.47}$
	Trans. w learnable tokens	$\mathbf{76.29} _{\pm \mathbf{0.51}}$	$\mathbf{80.80} _{\pm \mathbf{0.42}}$

able tokens and task-relatedness in formulating transformer-structured inference modules, which reduces negative transfer among heterogeneous tasks in each meta-test episode. Moreover, the variants with probabilistic inference modules consistently beat deterministic ones in performance, demonstrating the advantages of considering uncertainty during modeling and inference.

Effects of Different Ways to Generate Local Latent Parameters. We investigate the effects of different ways to generate each $\mathbf{w}_{\tau,o}^{m}$ from the shared condition $\mathbf{z}_{\tau}^{m}$ and $\mathcal{C}_{\tau}^{1:M}$. Given a Monte Carlo sample of global latent variables as $\mathbf{z}_{\tau}^{m(i)}$, in Table 5, we compare with two alternatives:

Table 5: **Performance comparisons of different implementations of generating each local latent parameter $\mathbf{w}_{\tau,o}^{m}$ from the condition $\mathbf{z}_{\tau}^{m}$ and $\mathcal{C}_{\tau}^{1:M}$.**

Methods	A	C	P	R	Avg.
Concat	$65.69 _{\pm 0.59}$	$58.64 _{\pm 0.61}$	$77.54 _{\pm 0.68}$	$77.10 _{\pm 0.64}$	$69.74 _{\pm 0.51}$
Add	$69.92 _{\pm 0.69}$	$63.73 _{\pm 0.71}$	$78.81 _{\pm 0.77}$	$79.03 _{\pm 0.78}$	$72.87 _{\pm 0.61}$
Ours	$\mathbf{73.31} _{\pm \mathbf{0.63}}$	$\mathbf{64.92} _{\pm \mathbf{0.68}}$	$\mathbf{83.38} _{\pm \mathbf{0.66}}$	$\mathbf{83.54} _{\pm \mathbf{0.64}}$	$\mathbf{76.29} _{\pm \mathbf{0.51}}$

1) Concat directly concatenates each context feature and $\mathbf{z}_{\tau}^{m(i)}$, and takes the concatenation as inputs of the transformer-structured inference network ϕ. 2) Add sums up each context feature and $\mathbf{z}_{\tau}^{m(i)}$ and takes the result as the input. 3) Ours incorporates $\mathbf{z}_{\tau}^{m(i)}$ into the transformer-structured inference module by merging it with the refined learnable tokens in Eq. (10). As shown in Table 5, Ours consistently performs the best. This implies that incorporating the conditional variables into the inference module is more effective than the direct combinations of $\mathbf{z}_{\tau}^{m(i)}$ and instance features.

Effects of More "Shots" or "Classes". To investigate the effects of more "shots" or "classes" in the episodic multi-task classification setup, we conduct experiments by increasing K or O in the defined M-task O-way K-shot setup.

As shown in Table 6, the proposed HNPs have more advantages over the baseline method with the context data points below ten shots. With shots larger than ten, both methods will reach a performance bottleneck.

Table 6: **Performance comparisons on Office-Home under the 4-task 5-way K-shot setup.**

Methods	1-shot	5-shot	10-shot	20-shot
TNP-D	$65.49 _{\pm 0.53}$	$78.94 _{\pm 0.43}$	$80.81 _{\pm 0.32}$	$81.12 _{\pm 0.68}$
HNPs	$76.29 _{\pm 0.51}$	$80.80 _{\pm 0.42}$	$81.28 _{\pm 0.38}$	$81.56 _{\pm 0.36}$

Moreover, Table 7 shows that our method consistently outperforms the baseline method as the number of classes increases from 20 to 40 in step 5. However, the performance gap between them narrows slightly with more classes. The main reason could be that the setting with more classes suffers from less data insufficiency.

Table 7: **Performance comparisons on `DomainNet` under the `6-task O-way 1-shot` setup.**

Methods	5-way	20-way	25-way	30-way	35-way	40-way
TNP-D	49.10 ± 0.42	28.83 ± 0.17	25.93 ± 0.14	24.08 ± 0.12	22.62 ± 0.11	21.64 ± 0.53
HNPs	62.36 ± 0.53	39.32 ± 0.23	35.72 ± 0.19	32.27 ± 0.17	31.27 ± 0.14	29.31 ± 0.13

Sensitivity to the Number of Monte Carlo Samples. For the hierarchical latent variables in the HNPs, we investigate the model's sensitivity to the number of Monte Carlo samples. Specifically, the sampling number of the global latent representation $\mathbf{z}_\tau^m$ and local latent parameters $\mathbf{w}_{\tau,1:O}^m$ varies from 1 to 30. We examine on `Office-Home` under the `4-task 5-way 1-shot` setting. In Figure 5, the runtime per iteration grows rapidly as the number of samples increases. However, there is no clear correlation between the performance and the num-

Figure 5: **Average accuracy and runtime of HNPs with different numbers of Monte Carlo samples.** N_z and N_w are sampling numbers of $\mathbf{z}_\tau^m$ and $\mathbf{w}_{\tau,1:O}^m$, respectively.

ber of Monte Carlo samples. There are two sweet spots in terms of average accuracy, one of which has favorable computation time. Hence, we set N_z and N_w to 5 and 10, respectively.

We also investigate the inference time of NP-based models per iteration on `Office-Home` under the 4task5way1shot setup. As shown in Table 8, our model needs more inference time than other NP-based meth-

Table 8: **Inference time of different NP-based methods.**

Methods	CNPs	NPs	TNP-D	HNPs
Inference time(s)	0.04	0.05	0.08	0.15

ods for performance gains. The cost mainly comes from inferring the designed hierarchical latent variables; however, we consider this a worthwhile trade-off for the extra performance.
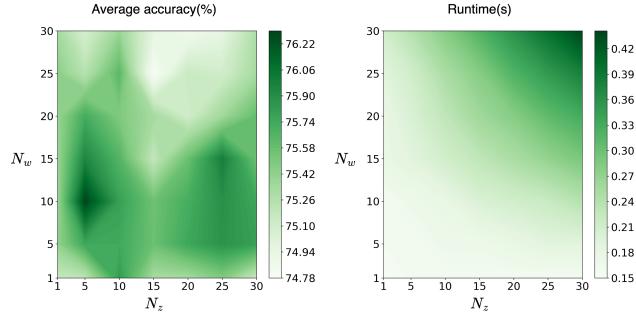
5   Conclusion

Technical Discussion. This work develops heterogeneous neural processes by introducing hierarchical latent variables and transformer-structured inference modules for episodic multi-task learning. With the help of heterogeneous context information and meta-knowledge, the proposed model can exploit task-relatedness, reason about predictive function distributions, and efficiently distill past knowledge to unseen heterogeneous tasks with limited data.

Limitation & Extension. Although the hierarchical probabilistic framework could mitigate the expressiveness bottleneck, the model needs more inference time than other NP-based methods for performance gains. Besides, the proposed method requires the target space to be the same across all tasks in a single episode. This requirement could limit the method's applicability in realistic scenarios where target spaces may differ across tasks. Our work could be extended to the new case without the shared target spaces, where the model should construct higher-order task-relatedness to improve knowledge sharing among tasks. Our code [3] is provided to facilitate such extensions.

Acknowledgment

---

[3] https://github.com/autumn9999/HNPs.git

References

[1] Ian Goodfellow, Yoshua Bengio, and Aaron Courville. *Deep Learning*. MIT Press, 2016. `http://www.deeplearningbook.org`.

[2] Shichao Xu, Lixu Wang, Yixuan Wang, and Qi Zhu. Weak adaptation learning: Addressing cross-domain data insufficiency with weak annotator. In *IEEE Conference on Computer Vision and Pattern Recognition*, 2021.

[3] Justin M Johnson and Taghi M Khoshgoftaar. Survey on deep learning with class imbalance. *Journal of Big Data*, 6(1):1–54, 2019.

[4] Oriol Vinyals, Charles Blundell, Timothy Lillicrap, Daan Wierstra, et al. Matching networks for one shot learning. In *Advances in Neural Information Processing Systems*, 2016.

[5] Chelsea Finn, Pieter Abbeel, and Sergey Levine. Model-agnostic meta-learning for fast adaptation of deep networks. In *International Conference on Machine Learning*, 2017.

[6] Jake Snell, Kevin Swersky, and Richard Zemel. Prototypical networks for few-shot learning. In *Advances in Neural Information Processing Systems*, 2017.

[7] James Requeima, Jonathan Gordon, John Bronskill, Sebastian Nowozin, and Richard E Turner. Fast and flexible multi-task classification using conditional neural adaptive processes. In *Advances in Neural Information Processing Systems*, 2019.

[8] Rich Caruana. Multitask learning. *Machine learning*, 28(1):41–75, 1997.

[9] Yu Zhang and Qiang Yang. A survey on multi-task learning. *IEEE Transactions on Knowledge and Data Engineering*, 2021.

[10] Mingsheng Long, Zhangjie Cao, Jianmin Wang, and S Yu Philip. Learning multiple tasks with multilinear relationship networks. In *Advances in neural information processing systems*, 2017.

[11] Jiayi Shen, Xiantong Zhen, Marcel Worring, and Ling Shao. Variational multi-task learning with gumbel-softmax priors. In *Advances in Neural Information Processing Systems*, 2021.

[12] Marta Garnelo, Jonathan Schwarz, Dan Rosenbaum, Fabio Viola, Danilo J Rezende, SM Eslami, and Yee Whye Teh. Neural processes. *arXiv preprint arXiv:1807.01622*, 2018.

[13] Marta Garnelo, Dan Rosenbaum, Christopher Maddison, Tiago Ramalho, David Saxton, Murray Shanahan, Yee Whye Teh, Danilo Rezende, and SM Ali Eslami. Conditional neural processes. In *International Conference on Machine Learning*, 2018.

[14] Wessel Bruinsma, Stratis Markou, James Requeima, Andrew Y. K. Foong, Tom Andersson, Anna Vaughan, Anthony Buonomo, Scott Hosking, and Richard E Turner. Autoregressive conditional neural processes. In *International Conference on Learning Representations*, 2023.

[15] Hyunjik Kim, Andriy Mnih, Jonathan Schwarz, Marta Garnelo, Ali Eslami, Dan Rosenbaum, Oriol Vinyals, and Yee Whye Teh. Attentive neural processes. In *International Conference on Learning Representations*, 2019.

[16] Qi Wang and Herke van Hoof. Learning expressive meta-representations with mixture of expert neural processes. In *Advances in Neural Information Processing Systems*, 2022.

[17] Sachin Ravi and Hugo Larochelle. Optimization as a model for few-shot learning. In *International Conference on Learning Representations*, 2017.

[18] Qi Wang and Herke Van Hoof. Doubly stochastic variational inference for neural processes with hierarchical latent variables. In *International Conference on Machine Learning*, 2020.

[19] Donggyun Kim, Seongwoong Cho, Wonkwang Lee, and Seunghoon Hong. Multi-task processes. *arXiv preprint arXiv:2110.14953*, 2021.

[20] Zongyu Guo, Cuiling Lan, Zhizheng Zhang, Yan Lu, and Zhibo Chen. Versatile neural processes for learning implicit neural representations. In *International Conference on Learning Representations*, 2023.

[21] Achim Klenke. *Probability theory: a comprehensive course*. Springer Science & Business Media, 2013.

[22] Wonjae Kim, Bokyung Son, and Ildoo Kim. Vilt: Vision-and-language transformer without convolution or region supervision. In *International Conference on Machine Learning*, 2021.

[23] Casper Kaae Sønderby, Tapani Raiko, Lars Maaløe, Søren Kaae Sønderby, and Ole Winther. Ladder variational autoencoders. In *Advances in Neural Information Processing Systems*, 2016.

[24] Alex Kendall, Yarin Gal, and Roberto Cipolla. Multi-task learning using uncertainty to weigh losses for scene geometry and semantics. In *IEEE Conference on Computer Vision and Pattern Recognition*, 2018.

[25] Shikun Liu, Edward Johns, and Andrew J Davison. End-to-end multi-task learning with attention. In *IEEE Conference on Computer Vision and Pattern Recognition*, 2019.

[26] Ishan Misra, Abhinav Shrivastava, Abhinav Gupta, and Martial Hebert. Cross-stitch networks for multi-task learning. In *IEEE Conference on Computer Vision and Pattern Recognition*, 2016.

[27] Liyang Liu, Yi Li, Zhanghui Kuang, Jing-Hao Xue, Yimin Chen, Wenming Yang, Qingmin Liao, and Wayne Zhang. Towards impartial multi-task learning. In *International Conference on Learning Representations*, 2020.

[28] Ozan Sener and Vladlen Koltun. Multi-task learning as multi-objective optimization. In *Advances in Neural Information Processing Systems*, 2018.

[29] Amir R Zamir, Alexander Sax, William Shen, Leonidas J Guibas, Jitendra Malik, and Silvio Savarese. Taskonomy: Disentangling task transfer learning. In *Proceedings of the IEEE conference on computer vision and pattern recognition*, 2018.

[30] Deblina Bhattacharjee, Tong Zhang, Sabine Süsstrunk, and Mathieu Salzmann. Mult: an end-to-end multitask learning transformer. In *Proceedings of the IEEE/CVF Conference on Computer Vision and Pattern Recognition*, 2022.

[31] Yi Zhang, Yu Zhang, and Wei Wang. Multi-task learning via generalized tensor trace norm. In *Proceedings of the 27th ACM SIGKDD Conference on Knowledge Discovery & Data Mining*, 2021.

[32] Jiayi Shen, Zehao Xiao, Xiantong Zhen, Cees GM Snoek, and Marcel Worring. Association graph learning for multi-task classification with category shifts. *arXiv preprint arXiv:2210.04637*, 2022.

[33] Yunlong Liang, Fandong Meng, Jinan Xu, Yufeng Chen, and Jie Zhou. Scheduled multi-task learning for neural chat translation. *arXiv preprint arXiv:2205.03766*, 2022.

[34] Yi Zhang, Yu Zhang, and Wei Wang. Learning linear and nonlinear low-rank structure in multi-task learning. *IEEE Transactions on Knowledge and Data Engineering*, 2022.

[35] Bart Bakker and Tom Heskes. Task clustering and gating for bayesian multitask learning. *Journal of Machine Learning Research*, 2003.

[36] Kai Yu, Volker Tresp, and Anton Schwaighofer. Learning gaussian processes from multiple tasks. In *International Conference on Machine Learning*, 2005.

[37] Michalis K Titsias and Miguel Lázaro-Gredilla. Spike and slab variational inference for multi-task and multiple kernel learning. In *Advances in neural information processing systems*, 2011.

[38] Neil D Lawrence and John C Platt. Learning to learn with the informative vector machine. In *International Conference on Machine Learning*, 2004.

[39] Fariba Yousefi, Michael Thomas Smith, and Mauricio A Álvarez. Multi-task learning for aggregated data using gaussian processes. *arXiv preprint arXiv:1906.09412*, 2019.

[40] Diane Oyen and Terran Lane. Leveraging domain knowledge in multitask bayesian network structure learning. In *Proceedings of the AAAI Conference on Artificial Intelligence*, 2012.

[41] Weizhu Qian, Bowei Chen, Yichao Zhang, Guanghui Wen, and Franck Gechter. Multi-task variational information bottleneck. *arXiv preprint arXiv:2007.00339*, 2020.

[42] Gjorgji Strezoski, Nanne van Noord, and Marcel Worring. Learning task relatedness in multi-task learning for images in context. In *International Conference on Multimedia Retrieval*, 2019.

[43] Ximeng Sun, Rameswar Panda, Rogerio Feris, and Kate Saenko. Adashare: Learning what to share for efficient deep multi-task learning. *arXiv preprint arXiv:1911.12423*, 2019.

[44] Gjorgji Strezoski, Nanne van Noord, and Marcel Worring. Many task learning with task routing. In *IEEE International Conference on Computer Vision*, 2019.

[45] Tianhe Yu, Saurabh Kumar, Abhishek Gupta, Sergey Levine, Karol Hausman, and Chelsea Finn. Gradient surgery for multi-task learning. *arXiv preprint arXiv:2001.06782*, 2020.

[46] Bo Liu, Xingchao Liu, Xiaojie Jin, Peter Stone, and Qiang Liu. Conflict-averse gradient descent for multi-task learning. In *Advances in Neural Information Processing Systems*, 2021.

[47] Chris Fifty, Ehsan Amid, Zhe Zhao, Tianhe Yu, Rohan Anil, and Chelsea Finn. Efficiently identifying task groupings for multi-task learning. In *Advances in Neural Information Processing Systems*, 2021.

[48] Pengsheng Guo, Chen-Yu Lee, and Daniel Ulbricht. Learning to branch for multi-task learning. In *International Conference on Machine Learning*, 2020.

[49] Sebastian Thrun and Lorien Pratt. Learning to learn: Introduction and overview. In *Learning to learn*, pages 3–17. Springer, 1998.

[50] Timothy M Hospedales, Antreas Antoniou, Paul Micaelli, and Amos J Storkey. Meta-learning in neural networks: A survey. *IEEE Transactions on Pattern Analysis and Machine Intelligence*, 2021.

[51] Kelsey R Allen, Evan Shelhamer, Hanul Shin, and Joshua B Tenenbaum. Infinite mixture prototypes for few-shot learning. In *International Conference on Machine Learning*, 2019.

[52] Boris Oreshkin, Pau Rodríguez López, and Alexandre Lacoste. Tadam: Task dependent adaptive metric for improved few-shot learning. In *Advances in neural information processing systems*, 2018.

[53] Sung Whan Yoon, Jun Seo, and Jaekyun Moon. Tapnet: Neural network augmented with task-adaptive projection for few-shot learning. In *International Conference on Machine Learning*, 2019.

[54] Victor Garcia and Joan Bruna. Few-shot learning with graph neural networks. In *International Conference on Learning Representations*, 2018.

[55] Tianshi Cao, Marc Law, and Sanja Fidler. A theoretical analysis of the number of shots in few-shot learning. *arXiv preprint arXiv:1909.11722*, 2019.

[56] Eleni Triantafillou, Tyler Zhu, Vincent Dumoulin, Pascal Lamblin, Utku Evci, Kelvin Xu, Ross Goroshin, Carles Gelada, Kevin Swersky, Pierre-Antoine Manzagol, and Hugo Larochelle. Meta-dataset: A dataset of datasets for learning to learn from few examples. *arXiv preprint arXiv:1903.03096*, 2019.

[57] Flood Sung, Yongxin Yang, Li Zhang, Tao Xiang, Philip HS Torr, and Timothy M Hospedales. Learning to compare: Relation network for few-shot learning. In *IEEE Conference on Computer Vision and Pattern Recognition*, 2018.

[58] Alex Nichol, Joshua Achiam, and John Schulman. On first-order meta-learning algorithms. *arXiv preprint arXiv:1803.02999*, 2018.

[59] Andrei A Rusu, Dushyant Rao, Jakub Sygnowski, Oriol Vinyals, Razvan Pascanu, Simon Osindero, and Raia Hadsell. Meta-learning with latent embedding optimization. In *International Conference on Learning Representations*, 2019.

[60] Flood Sung, Li Zhang, Tao Xiang, Timothy Hospedales, and Yongxin Yang. Learning to learn: Meta-critic networks for sample efficient learning. *arXiv preprint arXiv:1706.09529*, 2017.

[61] Zhenguo Li, Fengwei Zhou, Fei Chen, and Hang Li. Meta-sgd: Learning to learn quickly for few-shot learning. *arXiv preprint arXiv:1707.09835*, 2017.

[62] Jonathan Gordon, John Bronskill, Matthias Bauer, Sebastian Nowozin, and Richard E Turner. Meta-learning probabilistic inference for prediction. In *International Conference on Learning Representations*, 2019.

[63] Harrison Edwards and Amos Storkey. Towards a neural statistician. *arXiv preprint arXiv:1606.02185*, 2016.

[64] Chelsea Finn, Kelvin Xu, and Sergey Levine. Probabilistic model-agnostic meta-learning. In *Advances in Neural Information Processing Systems*, 2018.

[65] Steindór Sæmundsson, Katja Hofmann, and Marc Peter Deisenroth. Meta reinforcement learning with latent variable gaussian processes. *arXiv preprint arXiv:1803.07551*, 2018.

[66] Sungyong Baik, Junghoon Oh, Seokil Hong, and Kyoung Mu Lee. Learning to forget for meta-learning via task-and-layer-wise attenuation. *IEEE Transactions on Pattern Analysis and Machine Intelligence*, 2021.

[67] Myungsub Choi, Janghoon Choi, Sungyong Baik, Tae Hyun Kim, and Kyoung Mu Lee. Test-time adaptation for video frame interpolation via meta-learning. *IEEE Transactions on Pattern Analysis and Machine Intelligence*, 2021.

[68] Aniruddh Raghu, Maithra Raghu, Samy Bengio, and Oriol Vinyals. Rapid learning or feature reuse? towards understanding the effectiveness of maml. *arXiv preprint arXiv:1909.09157*, 2019.

[69] Ying Wei, Peilin Zhao, and Junzhou Huang. Meta-learning hyperparameter performance prediction with neural processes. In *International Conference on Machine Learning*, 2021.

[70] Stratis Markou, James Requeima, Wessel P Bruinsma, Anna Vaughan, and Richard E Turner. Practical conditional neural processes via tractable dependent predictions. *arXiv preprint arXiv:2203.08775*, 2022.

[71] Zesheng Ye and Lina Yao. Contrastive conditional neural processes. In *IEEE Conference on Computer Vision and Pattern Recognition*, 2022.

[72] Mingyu Kim, Kyeongryeol Go, and Se-Young Yun. Neural processes with stochastic attention: Paying more attention to the context dataset. *arXiv preprint arXiv:2204.05449*, 2022.

[73] Qi Wang, Marco Federici, and Herke van Hoof. Bridge the inference gaps of neural processes via expectation maximization. In *International Conference on Learning Representations*, 2023.

[74] Xiaozhuang Song, Shun Zheng, Wei Cao, James Yu, and Jiang Bian. Efficient and effective multi-task grouping via meta learning on task combinations. *Advances in Neural Information Processing Systems*, 2022.

[75] Richa Upadhyay, Prakash Chandra Chhipa, Ronald Phlypo, Rajkumar Saini, and Marcus Liwicki. Multi-task meta learning: learn how to adapt to unseen tasks. In *2023 International Joint Conference on Neural Networks (IJCNN)*. IEEE, 2023.

[76] Haoxiang Wang, Han Zhao, and Bo Li. Bridging multi-task learning and meta-learning: Towards efficient training and effective adaptation. In *International Conference on Machine Learning*, 2021.

[77] Hung-Yu Tseng, Hsin-Ying Lee, Jia-Bin Huang, and Ming-Hsuan Yang. Cross-domain few-shot classification via learned feature-wise transformation. In *International Conference on Learning Representations*, 2020.

[78] Wei-Yu Chen, Yen-Cheng Liu, Zsolt Kira, Yu-Chiang Frank Wang, and Jia-Bin Huang. A closer look at few-shot classification. *arXiv preprint arXiv:1904.04232*, 2019.

[79] Yunhui Guo, Noel C Codella, Leonid Karlinsky, James V Codella, John R Smith, Kate Saenko, Tajana Rosing, and Rogerio Feris. A broader study of cross-domain few-shot learning. In *European Conference on Computer Vision*, 2020.

[80] Yingjun Du, Xiantong Zhen, Ling Shao, and Cees G M Snoek. MetaNorm: Learning to normalize few-shot batches across domains. In *International Conference on Learning Representations*, 2021.

[81] Debasmit Das, Sungrack Yun, and Fatih Porikli. Confess: A framework for single source cross-domain few-shot learning. In *International Conference on Learning Representations*, 2022.

[82] Wei-Hong Li, Xialei Liu, and Hakan Bilen. Cross-domain few-shot learning with task-specific adapters. In *Proceedings of the IEEE/CVF Conference on Computer Vision and Pattern Recognition*, pages 7161–7170, 2022.

[83] Risto Vuorio, Shao-Hua Sun, Hexiang Hu, and Joseph J Lim. Multimodal model-agnostic meta-learning via task-aware modulation. In *Advances in neural information processing systems*, 2019.

[84] Risto Vuorio, Shao-Hua Sun, Hexiang Hu, and Joseph J Lim. Toward multimodal model-agnostic meta-learning. In *arXiv preprint arXiv:1812.07172*, 2018.

[85] Huaxiu Yao, Ying Wei, Junzhou Huang, and Zhenhui Li. Hierarchically structured meta-learning. In *International Conference on Machine Learning*, 2019.

[86] Milad Abdollahzadeh, Touba Malekzadeh, and Ngai-Man Man Cheung. Revisit multimodal meta-learning through the lens of multi-task learning. In *Advances in Neural Information Processing Systems*, 2021.

[87] Jiayi Chen and Aidong Zhang. Hetmaml: Task-heterogeneous model-agnostic meta-learning for few-shot learning across modalities. In *Proceedings of the 30th ACM International Conference on Information & Knowledge Management*, 2021.

[88] Chen Xing, Negar Rostamzadeh, Boris Oreshkin, and Pedro O O Pinheiro. Adaptive cross-modal few-shot learning. In *Advances in Neural Information Processing Systems*, 2019.

[89] Frederik Pahde, Patrick Jähnichen, Tassilo Klein, and Moin Nabi. Cross-modal hallucination for few-shot fine-grained recognition. *arXiv preprint arXiv:1806.05147*, 2018.

[90] Frederik Pahde, Mihai Puscas, Tassilo Klein, and Moin Nabi. Multimodal prototypical networks for few-shot learning. In *Proceedings of the IEEE/CVF Winter Conference on Applications of Computer Vision*, 2021.

[91] Hemanth Venkateswara, Jose Eusebio, Shayok Chakraborty, and Sethuraman Panchanathan. Deep hashing network for unsupervised domain adaptation. In *IEEE Conference on Computer Vision and Pattern Recognition*, 2017.

[92] Xingchao Peng, Qinxun Bai, Xide Xia, Zijun Huang, Kate Saenko, and Bo Wang. Moment matching for multi-source domain adaptation. In *IEEE International Conference on Computer Vision*, 2019.

[93] Ishaan Gulrajani and David Lopez-Paz. In search of lost domain generalization. *arXiv preprint arXiv:2007.01434*, 2020.

[94] Ze Wang, Zichen Miao, Xiantong Zhen, and Qiang Qiu. Learning to learn dense gaussian processes for few-shot learning. In *Advances in Neural Information Processing Systems*, 2021.

[95] Tung Nguyen and Aditya Grover. Transformer neural processes: Uncertainty-aware meta learning via sequence modeling. *arXiv preprint arXiv:2207.04179*, 2022.

[96] Richa Upadhyay, Prakash Chandra Chhipa, Ronald Phlypo, Rajkumar Saini, and Marcus Liwicki. Multi-task meta learning: learn how to adapt to unseen tasks. *arXiv preprint arXiv:2210.06989*, 2022.

[97] Qianqian Zhang, Xinru Liao, Quan Liu, Jian Xu, and Bo Zheng. Leaving no one behind: A multi-scenario multi-task meta learning approach for advertiser modeling. In *Proceedings of the Fifteenth ACM International Conference on Web Search and Data Mining*, 2022.

[98] Kaidi Cao, Jiaxuan You, and Jure Leskovec. Relational multi-task learning: Modeling relations between data and tasks. In *International Conference on Learning Representations*, 2021.

[99] Huaiwen Zhang, Shengsheng Qian, Quan Fang, and Changsheng Xu. Multi-modal meta multi-task learning for social media rumor detection. *IEEE Transactions on Multimedia*, 24:1449–1459, 2021.

[100] Chu Han, Huasheng Yao, Bingchao Zhao, Zhenhui Li, Zhenwei Shi, Lei Wu, Xin Chen, Jinrong Qu, Ke Zhao, Rushi Lan, et al. Meta multi-task nuclei segmentation with fewer training samples. *Medical Image Analysis*, 2022.

[101] Guan-Yuan Chen and Ya-Fen Yeh. Mmtl: The meta multi-task learning for aspect category sentiment analysis. In *Proceedings of the 33rd Conference on Computational Linguistics and Speech Processing*, 2021.

[102] Alessandro Achille, Michael Lam, Rahul Tewari, Avinash Ravichandran, Subhransu Maji, Charless C Fowlkes, Stefano Soatto, and Pietro Perona. Task2vec: Task embedding for meta-learning. In *Proceedings of the IEEE/CVF international conference on computer vision*, 2019.

[103] Cuong C Nguyen, Thanh-Toan Do, and Gustavo Carneiro. Probabilistic task modelling for meta-learning. In *Uncertainty in Artificial Intelligence*, 2021.

[104] Diederik P Kingma and Max Welling. Auto-encoding variational bayes. *arXiv preprint arXiv:1312.6114*, 2013.

[105] Durk P Kingma, Tim Salimans, and Max Welling. Variational dropout and the local reparameterization trick. In *Advances in neural information processing systems*, 2015.

[106] Karen Simonyan and Andrew Zisserman. Very deep convolutional networks for large-scale image recognition. *arXiv preprint arXiv:1409.1556*, 2014.

[107] Kaiming He, Xiangyu Zhang, Shaoqing Ren, and Jian Sun. Deep residual learning for image recognition. In *Proceedings of the IEEE conference on computer vision and pattern recognition*, 2016.

[108] Diederik P Kingma and Jimmy Ba. Adam: A method for stochastic optimization. *arXiv preprint arXiv:1412.6980*, 2014.

[109] Huaxiu Yao, Linjun Zhang, and Chelsea Finn. Meta-learning with fewer tasks through task interpolation. *arXiv preprint arXiv:2106.02695*, 2021.

[110] Kate Saenko, Brian Kulis, Mario Fritz, and Trevor Darrell. Adapting visual category models to new domains. In *European Conference on Computer Vision*, 2010.

[111] Brian Kulis, Kate Saenko, and Trevor Darrell. What you saw is not what you get: Domain adaptation using asymmetric kernel transforms. In *CVPR 2011*. IEEE, 2011.

[112] Yann LeCun, Léon Bottou, Yoshua Bengio, and Patrick Haffner. Gradient-based learning applied to document recognition. *Proceedings of the IEEE*, 86(11):2278–2324, 1998.

[113] Boqing Gong, Yuan Shi, Fei Sha, and Kristen Grauman. Geodesic flow kernel for unsupervised domain adaptation. In *IEEE Conference on Computer Vision and Pattern Recognition*, 2012.

[114] Gregory Griffin, Alex Holub, and Pietro Perona. Caltech-256 object category dataset. *Dataset Report*, 2007.

[115] Mateusz Buda, Ashirbani Saha, and Maciej A Mazurowski. Association of genomic subtypes of lower-grade gliomas with shape features automatically extracted by a deep learning algorithm. *Computers in biology and medicine*, 109:218–225, 2019.

[116] Olaf Ronneberger, Philipp Fischer, and Thomas Brox. U-net: Convolutional networks for biomedical image segmentation. In *International Conference on Medical Image Computing and Computer-Assisted Intervention*, 2015.

Contents

A Frequently Asked Questions

In this section, we list frequently asked questions from researchers who help proofread this manuscript. These raised questions might also be relevant for others and help in better understanding the paper, so we include more detailed discussions here.

Connections between different settings. This work considers the multi-input multi-output setting of multi-task learning under the episodic training mechanism.

As shown in Table 9, we use "Heterogeneous tasks" to distinguish the different branches of multi-task learning: (1) *single-input multi-output* (SIMO) considers different tasks which have the same input and different supervision information. (2) *multi-input multi-output* (MIMO) considers heterogeneous tasks, which have different inputs and follow different data distributions. All tasks are related since they share the target space. This setting encourages deep models to deal with the insufficient data of each task by aggregating the training data from related tasks in the spirit of data augmentation.

Meanwhile, "Episodic training" is used to describe the data-feeding strategy. *Multi-task meta-learning* also benefits from episodic training, but it follows the SIMO setting in every single episode and cannot sufficiently handle heterogeneous tasks. In our work, *episodic multi-task learning* is designed based on the MIMO setting, suffering from distribution shifts between heterogeneous tasks. In addition, we note that *conventional meta-learning* follows the "Episodic training" mechanism but focuses on single-task learning in each episode. Thus, "Heterogeneous tasks" is not available here (-). More details are left in Table (9).

Table 9: **Connections between different settings.** The symbols ✓ and ✗ indicate whether or not the specific setting has the corresponding characteristic.

Settings	Methods	Episodic training	Heterogeneous tasks
single-input multi-output (SIMO)	[24–30]	✗	✗
multi-input multi-output (MIMO)	[11, 10, 31–34]	✗	✓
conventional meta-learning	[4–7, 12, 13]	✓	-
multi-task meta-learning	[96–98, 19, 99–101]	✓	✗
episodic multi-task learning	This paper	✓	✓

Problem scope. In episodic multi-task learning, we restrict the scope of the problem to the case where tasks in the same episode are related and share the same target space. There are two main reasons: (1) we follow the MIMO setting of multi-task learning in every single episode, where the same target space assures the existence of the knowledge shared among tasks. (2) As demonstrated in recent works [102, 103], meta-learning tasks generated from the same categories or taxonomic clusters are closer. This also implies that tasks with the same target space are related.

Differences from other episodic single-task setups. Based on episodic training, there are several approaches related to the setting of episodic multi-task learning: (1) *cross-domain few-shot learning* addresses few-shot learning under domain shifts [77]. Several models [78, 77, 79–82] train a model on a single source domain or several source domains and then generalize it to other domains. In contrast, our research emphasizes the domain shifts within individual episodes rather than among them. (2) *multimodal meta-learning* extends few-shot learning from a single input-label domain to multiple different input-label domains [83]. These methods [84, 83, 56, 85–87] design a meta-learner that can handle tasks from distinct distributions in sequence. Our work centers on simultaneously dealing with several related tasks within a meta-training or meta-test episode. (3) *cross-modality few-shot learning* [88–90] leverages semantic information (e.g., word vectors) to augment the performance of visual tasks and not among visual tasks only. The aforementioned approaches exclusively address single-task learning per episode, while our work concurrently tackles multiple heterogeneous and related tasks within each meta-training or meta-test episode. Intuitive comparisons with the approaches are shown in Figure 6.

Different roles of global and local latent variables. In this paper, we introduce global latent representations and local latent parameters within a hierarchical architecture. Each type of them plays a distinct role in the proposed model: (1) Global latent representations provide rich task-specific information during the inference of all local latent parameters. This enables the model to generate

Figure 6: **Differences from other episodic single-task setups**. Each row corresponds to an episode. Different color denotes different categories; the same color with different shades represents different categories in the same task. Episodic multi-task learning is orthogonal to these setups since it concurrently tackles multiple heterogeneous and related tasks within each episode.

task-specific decoders to handle heterogeneous tasks in a single episode effectively. (2) Local latent parameters with prediction-aware information constitute task-specific decoders. Each local latent parameter reveals the knowledge corresponding to a specific prediction across different tasks. This enhances the expressive power of the proposed model. In practice, we observe that global latent representations and local latent parameters complement each other when performing predictions in meta-test episodes.

Advantages of the proposed hierarchical Bayes framework. We summarize the advantages of the proposed framework. (1) A hierarchical Bayesian framework with global and local latent variables yields a richer and more complex latent space to mitigate the expressiveness bottleneck, thus better parameterizing task-specific functions in stochastic processes. (2) Global and local latent variables capture epistemic uncertainty in representation and parameter levels, respectively, and show improved performance in our experiments.

Roles of probabilistic HNPs and KL values in meta training. The probabilistic HNPs encode the context as the heterogeneous prior and reveal the uncertainty resulting from data insufficiency and the extent of observations in tasks. Additionally, minimizing KL terms encourages priors inferred from context sets to stay close to posteriors inferred from target sets, guiding more efficient conditional generation. In training processes, we observed the KL divergence value does not decrease to 0 after convergence, e.g., KL values are in the order of e-1 on Office-home. This is also part of traits in the NPs family, suggesting the approximate posterior and the approximate prior encode different conditional information during the generation of latent variables.

Real-world examples or benchmarks for episodic multi-task learning. Episodic multi-task learning has several potential applications in the real world, such as autonomous driving and robotic manipulations. In detail, the autonomous driving system needs to deal with different and related sensor data in an environment. However, the driving environment constantly changes along with the weather, time, country, etc. Thus, fast adapting of the current multi-tasker to new environments is challenging in this application and our method can be a plausible solution for this challenge.

B Properties of Valid Exchangeable Stochastic Processes

Here, we further demonstrate that HNPs are valid stochastic processes, as meeting the *exchangeability* and *marginalization* consistency conditions [12]. As stated in [12]: the conditions, including (finite) exchangeability and marginalization, are sufficient to define a stochastic process with the help of the Kolmogorov extension theorem. Here we follow the notations in the main paper. For convenience, we provide the used symbols and the corresponding descriptions in Table 10.

In this paper, we model the functional posterior distribution of the stochastic process by approximating the joint distribution over all target sets $p(\mathbf{y}_\tau^{1:M}|\mathbf{x}_\tau^{1:M}, \mathcal{C}_\tau^{1:M})$, which is conditioned on all context samples $C_\tau^{1:M}$. To distinguish the order set among different tasks, we use n_τ^m to denote the number of target samples corresponding to a specific task in the episode τ. For simplicity, we omit the meta-knowledge ω and $\nu^{1:M}$ in the formulations during the proof.

Table 10: Notations and their corresponding descriptions in this paper.

Notation	Description
$(\cdot)_\tau$	Variables correspond to an episode.
$(\cdot)^m$	Variables correspond to a single task.
$\mathcal{I}_\tau^m$	A single task in the episode τ, which is sampled from a specific task distribution.
$p(\mathcal{I}^m)$	The specific task distribution.
M	The number of task distributions and the number of tasks in a single episode.
$\mathcal{I}_\tau^{1:M}$	All heterogeneous tasks in the episode τ.
$\mathcal{C}$	A context set.
$\mathcal{T}$	A target set.
$\bar{x}$	A context sample feature of the context set.
x	A target sample feature of the target set.
$\mathbf{x}$	Set of all target sample features in the target set.
$\bar{y}$	The ground truth of the context sample.
y	The ground truth of the target sample.
$\mathbf{y}$	Set of the ground truth of all target samples in the target set.
$\mathcal{N}_\mathcal{C}$	The numbers of context samples in the context set.
$\mathcal{N}_\mathcal{T}$	The numbers of target samples in the target set.
$\mathbf{z}_\tau^m$	The introduced global latent representation for a given task.
$\mathbf{w}_{\tau,1:O}^m$	The introduced local latent parameters for a given task.

B.1 Proof of Exchangeability Consistency

We now provide the proof of *Exchangeability Consistency*: the joint prediction distribution is invariant to the permutation of the given multiple tasks and the corresponding samples in each task.

Theorem B.1. *(Exchangability) For finite* $n_\tau^* = \sum_{m=1}^M n_\tau^m$, *if* $\pi_\tau^* = \{\pi_\tau^m\}_{m=1}^M$ *is a permutation of* $\{1, \cdots, n^*\}$ *where* π_τ^m *is a permutation of the corresponding order set* $\{1, \cdots, n_\tau^m\}$, *then:*

$$p(\pi_\tau^*(\mathbf{y}_\tau^{1:M})|\pi_\tau^*(\mathbf{x}_\tau^{1:M}), \mathcal{C}_\tau^{1:M}) = p(\mathbf{y}_\tau^{1:M}|\mathbf{x}_\tau^{1:M}, \mathcal{C}_\tau^{1:M}),$$

where $\pi_\tau^*(\mathbf{y}_\tau^{1:M}) := (\pi_\tau^1(\mathbf{y}_\tau^1), \cdots, \pi_\tau^M(\mathbf{y}_\tau^M)) = (y_{\tau,\pi_\tau^*(1)}, \cdots, y_{\tau,\pi_\tau^*(n_\tau^*)})$ *and* $\pi_\tau^*(\{\mathbf{x}_\tau^{1:M}\}) := (\pi_\tau^1(\mathbf{x}_\tau^1), \cdots, \pi_\tau^M(\mathbf{x}_\tau^M)) = (x_{\tau,\pi_\tau^*(1)}, \cdots, x_{\tau,\pi_\tau^*(n_\tau^*)})$.

Proof.

$$p(\pi_\tau^*(\mathbf{y}_\tau^{1:M})|\pi_\tau^*(\mathbf{x}_\tau^{1:M}), \mathcal{C}_\tau^{1:M})$$

$$= \int\int p(\pi_\tau^*(\mathbf{y}_\tau^{1:M})|\pi_\tau^*(\mathbf{x}_\tau^{1:M}), \mathbf{w}_{\tau,1:O}^{1:M})\Big(\prod_{m=1}^M p(\mathbf{w}_{\tau,1:O}^m|\mathbf{z}_\tau^m, \mathcal{C}_\tau^{1:M})\Big)\Big(\prod_{m=1}^M p(\mathbf{z}_\tau^m|\mathcal{C}_\tau^m)\Big)d\mathbf{w}_{\tau,1:O}^{1:M}d\mathbf{z}_\tau^{1:M}$$

$$= \int\int \Big(\prod_{i=1}^{n_\tau^*} p(y_{\tau,\pi_\tau^*(i)}|x_{\tau,\pi_\tau^*(i)}, \mathbf{w}_{\tau,1:O}^{1:M})\Big)\Big(\prod_{m=1}^M p(\mathbf{w}_{\tau,1:O}^m|\mathbf{z}_\tau^m, \mathcal{C}_\tau^{1:M})\Big)\Big(\prod_{m=1}^M p(\mathbf{z}_\tau^m|\mathcal{C}_\tau^m)\Big)d\mathbf{w}_{\tau,1:O}^{1:M}d\mathbf{z}_\tau^{1:M}$$

$$= \int\int \prod_{m=1}^M\Big\{\prod_{j=1}^{n_\tau^m} p(y_{\tau,\pi_\tau^m(j)}^m|x_{\tau,\pi_\tau^m(j)}^m, \mathbf{w}_{\tau,1:O}^m)p(\mathbf{w}_{\tau,1:O}^m|\mathbf{z}_\tau^m, \mathcal{C}_\tau^{1:M})p(\mathbf{z}_\tau^m|\mathcal{C}_\tau^m)\Big\}d\mathbf{w}_{\tau,1:O}^{1:M}d\mathbf{z}_\tau^{1:M}$$

$$= \int\int \prod_{m=1}^M\Big\{\prod_{j=1}^{n_\tau^m} p(y_{\tau,j}^m|x_{\tau,j}^m, \mathbf{w}_{\tau,1:O}^m)p(\mathbf{w}_{\tau,1:O}^m|\mathbf{z}_\tau^m, \mathcal{C}_\tau^{1:M})p(\mathbf{z}_\tau^m|\mathcal{C}_\tau^m)\Big\}d\mathbf{w}_{\tau,1:O}^{1:M}d\mathbf{z}_\tau^{1:M}$$

$$= p(\mathbf{y}_\tau^{1:M}|\mathbf{x}_\tau^{1:M}, \mathcal{C}_\tau^{1:M}).$$

$\square$

B.2 Proof of Marginalization Consistency

We now aim to prove the *Marginalization Consistency* of the proposed model: if marginalizing out a part of the target set in each task, the marginal distribution remains the same as defined on the original target sets without the marginalized part.

Theorem B.2. *(Marginalization) Given* $\hat{n}_\tau^* = \sum_{m=1}^M \hat{n}_\tau^m$, *where* $1 \leq \hat{n}_\tau^* \leq n_\tau^*$ *and for each task* $1 \leq \hat{n}_\tau^m \leq n_\tau^m$, *the consistency is:*

$$\int p(\mathbf{y}_\tau^{1:M}|\mathbf{x}_\tau^{1:M}, \mathcal{C}_\tau^{1:M})d(\mathbf{y}_\tau^{1:M})_{\hat{n}_\tau^*+1:n_\tau^*} = p((\mathbf{y}_\tau^{1:M})_{1:\hat{n}_\tau^*}|(\mathbf{x}_\tau^{1:M})_{1:\hat{n}_\tau^*}, \mathcal{C}_\tau^{1:M}),$$

where $(\mathbf{y}_\tau^{1:M})_{1:\hat{n}_\tau^*} = ((\mathbf{y}_\tau^1)_{1:\hat{n}_\tau^1}, \cdots, (\mathbf{y}_\tau^M)_{1:\hat{n}_\tau^M}) = (y_{\tau,1}, \cdots, y_{\tau,\hat{n}_\tau^*})$ *and* $(\mathbf{x}_\tau^{1:M})_{1:\hat{n}_\tau^*} = ((\mathbf{x}_\tau^1)_{1:\hat{n}_\tau^1}, \cdots, (\mathbf{x}_\tau^M)_{1:\hat{n}_\tau^M}) = (x_{\tau,1}, \cdots, x_{\tau,\hat{n}_\tau^*})$.

Proof.

$$\int p(\mathbf{y}_\tau^{1:M}|\mathbf{x}_\tau^{1:M}, \mathcal{C}_\tau^{1:M})d(\mathbf{y}_\tau^{1:M})_{\hat{n}_\tau^*+1:n_\tau^*}$$

$$= \int\int\int p(\mathbf{y}_\tau^{1:M}|\mathbf{x}_\tau^{1:M}, \mathbf{w}_{\tau,1:O}^{1:M})\Big(\prod_{m=1}^M p(\mathbf{w}_{\tau,1:O}^m|\mathbf{z}_\tau^m, \mathcal{C}_\tau^{1:M})\Big)\Big(\prod_{m=1}^M p(\mathbf{z}_\tau^m|\mathcal{C}_\tau^m)\Big)d\mathbf{w}_{\tau,1:O}^{1:M}d\mathbf{z}_\tau^{1:M}d(\mathbf{y}_\tau^{1:M})_{\hat{n}_\tau^*+1:n_\tau^*}$$

$$= \int\int\int \Big(\prod_{i=1}^{n_\tau^*} p(y_{\tau,i}|x_{\tau,i}, \mathbf{w}_{\tau,1:O}^{1:M})\Big)\Big(\prod_{m=1}^M p(\mathbf{w}_{\tau,1:O}^m|\mathbf{z}_\tau^m, \mathcal{C}_\tau^{1:M})\Big)\Big(\prod_{m=1}^M p(\mathbf{z}_\tau^m|\mathcal{C}_\tau^m)\Big)d\mathbf{w}_{\tau,1:O}^{1:M}d\mathbf{z}_\tau^{1:M}d(\mathbf{y}_\tau^{1:M})_{\hat{n}_\tau^*+1:n_\tau^*}$$

$$= \int\int \prod_{m=1}^M\Big\{\int\prod_{j=1}^{n_\tau^m} p(y_{\tau,j}^m|x_{\tau,j}^m, \mathbf{w}_{\tau,1:O}^m)p(\mathbf{w}_{\tau,1:O}^m|\mathbf{z}_\tau^m, \mathcal{C}_\tau^{1:M})p(\mathbf{z}_\tau^m|\mathcal{C}_\tau^m)d(\mathbf{y}_\tau^m)_{\hat{n}_\tau^m+1:n_\tau^m}\Big\}d\mathbf{w}_{\tau,1:O}^{1:M}d\mathbf{z}_\tau^{1:M}$$

$$= \int\int \prod_{m=1}^M\Big\{\prod_{j=1}^{\hat{n}_\tau^m} p(y_{\tau,j}^m|x_{\tau,j}^m, \mathbf{w}_{\tau,1:O}^m)p(\mathbf{w}_{\tau,1:O}^m|\mathbf{z}_\tau^m, \mathcal{C}_\tau^{1:M})p(\mathbf{z}_\tau^m|\mathcal{C}_\tau^m)$$

$$\int\prod_{j=\hat{n}_\tau^m+1}^{n_\tau^m} p(y_{\tau,j}^m|x_{\tau,j}^m, \mathbf{w}_{\tau,1:O}^m)d(\mathbf{y}_\tau^m)_{\hat{n}_\tau^m+1:n_\tau^m}\Big\}d\mathbf{w}_{\tau,1:O}^{1:M}d\mathbf{z}_\tau^{1:M}$$

$$= \int\int \prod_{m=1}^M\Big\{\prod_{j=1}^{\hat{n}_\tau^m} p(y_{\tau,j}^m|x_{\tau,j}^m, \mathbf{w}_{\tau,1:O}^m)p(\mathbf{w}_{\tau,1:O}^m|\mathbf{z}_\tau^m, \mathcal{C}_\tau^{1:M})p(\mathbf{z}_\tau^m|\mathcal{C}_\tau^m)\Big\}d\mathbf{w}_{\tau,1:O}^{1:M}d\mathbf{z}_\tau^{1:M}$$

$$= p((\mathbf{y}_\tau^{1:M})_{1:\hat{n}_\tau^*}|(\mathbf{x}_\tau^{1:M})_{1:\hat{n}_\tau^*}, \mathcal{C}_\tau^{1:M}).$$

$\square$

C Tractable and Scalable Optimization

For the proposed HNPs, it is intractable to obtain the true joint posterior $p(\mathbf{w}_{\tau,1:O}^{1:M}, \mathbf{z}_\tau^{1:M} | \mathcal{T}_\tau^{1:M}; \omega, \nu^{1:M})$ for each episode. Thus, we employ variational inference to optimize the designed model by approximating the true joint posterior in each episode. To do so, we introduce the variational joint posterior distribution:

$$q_{\theta,\phi}(\mathbf{w}_{\tau,1:O}^{1:M}, \mathbf{z}_\tau^{1:M} | \mathcal{T}_\tau^{1:M}; \omega, \nu^{1:M}) = \prod_{m=1}^{M} q_\theta(\mathbf{z}_\tau^m | \mathcal{T}_\tau^m; \nu^m) q_\phi(\mathbf{w}_{\tau,1:O}^m | \mathbf{z}_\tau^m, \mathcal{T}_\tau^{1:M}; \omega), \quad (11)$$

where $q_\theta(\mathbf{z}_\tau^m | \mathcal{T}_\tau^m; \nu^m)$ and $q_\phi(\mathbf{w}_{\tau,1:O}^m | \mathbf{z}_\tau^m, \mathcal{T}_\tau^{1:M}; \omega)$ are variational posteriors of their corresponding latent variables. We note that variational posteriors are inferred from the target sets that are available in the meta-training stage. The variational posteriors are parameterized as diagonal Gaussian distributions [104]. The inference networks θ and ϕ are shared by the variational posteriors and their corresponding priors, following the protocol of vanilla NPs [12].

C.1 Derivation of Approximate ELBO for HNPs

By incorporating the variational posteriors in Eq. (11) into the modeling of HNPs in the main paper, we can derive the approximate ELBO $L_{\text{HNPs}}(\omega, \nu^{1:M}, \theta, \phi)$ as follows:

$$\log p(\mathcal{T}_\tau^{1:M} | \mathcal{C}_\tau^{1:M}; \omega, \nu^{1:M})$$

$$= \sum_{m=1}^{M} \log p(\mathcal{T}_\tau^m | \mathcal{C}_\tau^{1:M}; \omega, \nu^m)$$

$$= \sum_{m=1}^{M} \left\{ \log \int \left\{ \int p(\mathbf{y}_\tau^m | \mathbf{x}_\tau^m, \mathbf{w}_{\tau,1:O}^m) p_\phi(\mathbf{w}_{\tau,1:O}^m | \mathbf{z}_\tau^m, \mathcal{C}_\tau^{1:M}; \omega) d\mathbf{w}_{\tau,1:O}^m \right\} p_\theta(\mathbf{z}_\tau^m | \mathcal{C}_\tau^m; \nu^m) d\mathbf{z}_\tau^m \right\}$$

$$= \sum_{m=1}^{M} \left\{ \log \int \left\{ \int p(\mathbf{y}_\tau^m | \mathbf{x}_\tau^m, \mathbf{w}_{\tau,1:O}^m) p_\phi(\mathbf{w}_{\tau,1:O}^m | \mathbf{z}_\tau^m, \mathcal{C}_\tau^{1:M}; \omega) \frac{q_\phi(\mathbf{w}_{\tau,1:O}^m | \mathbf{z}_\tau^m, \mathcal{T}_\tau^{1:M}; \omega)}{q_\phi(\mathbf{w}_{\tau,1:O}^m | \mathbf{z}_\tau^m, \mathcal{T}_\tau^{1:M}; \omega)} d\mathbf{w}_{\tau,1:O}^m \right\} \right.$$

$$\left. p_\theta(\mathbf{z}_\tau^m | \mathcal{C}_\tau^m; \nu^m) \frac{q_\theta(\mathbf{z}_\tau^m | \mathcal{T}_\tau^m; \nu^m)}{q_\theta(\mathbf{z}_\tau^m | \mathcal{T}_\tau^m; \nu^m)} d\mathbf{z}_\tau^m \right\}$$

$$\geq \sum_{m=1}^{M} \left\{ \mathbb{E}_{q_\theta(\mathbf{z}_\tau^m | \mathcal{T}_\tau^m; \nu^m)} \left\{ \log \int p(\mathbf{y}_\tau^m | \mathbf{x}_\tau^m, \mathbf{w}_{\tau,1:O}^m) p_\phi(\mathbf{w}_{\tau,1:O}^m | \mathbf{z}_\tau^m, \mathcal{C}_\tau^{1:M}; \omega) \frac{q_\phi(\mathbf{w}_{\tau,1:O}^m | \mathbf{z}_\tau^m, \mathcal{T}_\tau^{1:M}; \omega)}{q_\phi(\mathbf{w}_{\tau,1:O}^m | \mathbf{z}_\tau^m, \mathcal{T}_\tau^{1:M}; \omega)} d\mathbf{w}_{\tau,1:O}^m \right\} \right.$$

$$\left. - \mathbb{D}_{\text{KL}}[q_\theta(\mathbf{z}_\tau^m | \mathcal{T}_\tau^m; \nu^m) || p_\theta(\mathbf{z}_\tau^m | \mathcal{C}_\tau^m; \nu^m)] \right\}$$

$$\geq \sum_{m=1}^{M} \left\{ \mathbb{E}_{q_\theta(\mathbf{z}_\tau^m | \mathcal{T}_\tau^m; \nu^m)} \left\{ \mathbb{E}_{q_\phi(\mathbf{w}_{\tau,1:O}^m | \mathbf{z}_\tau^m, \mathcal{T}_\tau^{1:M}; \omega)} [\log p(\mathbf{y}_\tau^m | \mathbf{x}_\tau^m, \mathbf{w}_{\tau,1:O}^m)] \right. \right.$$

$$\left. - \mathbb{D}_{\text{KL}}[q_\phi(\mathbf{w}_{\tau,1:O}^m | \mathbf{z}_\tau^m, \mathcal{T}_\tau^{1:M}; \omega) || p_\phi(\mathbf{w}_{\tau,1:O}^m | \mathbf{z}_\tau^m, \mathcal{C}_\tau^{1:M}; \omega)] \right\}$$

$$\left. - \mathbb{D}_{\text{KL}}[q_\theta(\mathbf{z}_\tau^m | \mathcal{T}_\tau^m; \nu^m) || p_\theta(\mathbf{z}_\tau^m | \mathcal{C}_\tau^m; \nu^m)] \right\} = L_{\text{HNPs}}(\omega, \nu^{1:M}, \theta, \phi).$$

$$(12)$$

In general, when the variational joint posterior is flexible enough, the posterior approximation gap between the variational posterior and the intractable true posterior can be reduced to an arbitrarily small quantity [73]. In this case, maximizing the approximate ELBO increases the overall log likelihood in the proposed model accordingly. We construct task-specific decoders in a data-driven way by inferring local latent parameters $\mathbf{w}_{1:O}^m$ from all context sets and the meta-knowledge. This enables our model to amortize the training cost of each task-specific decoder, further reducing the model's over-fitting behaviors for episodic multi-task learning.

C.2 Meta-Training Objective

In practice, we consider the loss function as the negative approximate ELBO of HNPs as given in Eq. (12). By adopting Monte Carlo sampling [104, 105], the meta-training objective for each episode

is:

$$-L_{\text{HNPs}}(\omega, \nu^{1:M}, \theta, \phi) \approx \sum_{m=1}^{M} \left\{ \frac{1}{N_z} \sum_{i=1}^{N_z} \left\{ \frac{1}{N_w} \sum_{j=1}^{N_w} [-\log p(\mathbf{y}_\tau^m | \mathbf{x}_\tau^m, \mathbf{w}_{\tau,1:O}^{m}{}^{(j)})] \right. \right.$$
$$\left. + \mathbb{D}_{\text{KL}}[q_\phi(\mathbf{w}_{\tau,1:O}^{m} | \mathbf{z}_\tau^{m(i)}, \mathcal{T}_\tau^{1:M}; \omega) || p_\phi(\mathbf{w}_{\tau,1:O}^{m} | \mathbf{z}_\tau^{m(i)}, \mathcal{C}_\tau^{1:M}; \omega)] \right\} \tag{13}$$
$$\left. + \mathbb{D}_{\text{KL}}[q_\theta(\mathbf{z}_\tau^m | \mathcal{T}_\tau^m; \nu^m) || p_\theta(\mathbf{z}_\tau^m | \mathcal{C}_\tau^m; \nu^m)] \right\},$$

where $\mathbf{z}_\tau^{m(i)}$ and $\mathbf{w}_{\tau,1:O}^{m}{}^{(j)}$ are sampled from their corresponding variational posteriors. N_z and N_w are the number of Monte Carlo samples for $\mathbf{z}_\tau^m$ and $\mathbf{w}_{\tau,1:O}^{m}$, respectively.

C.3 Meta-Test Prediction

At the meta-test stage, we perform predictions with the learned model on the target sets for a new episode τ^*, which involves the prior distributions of global and local latent variables. We again approximate the predictive distribution with Monte Carlo estimates:

$$p(\mathcal{T}_{\tau^*}^{1:M} | \mathcal{C}_{\tau^*}^{1:M}; \omega, \nu^{1:M}) \approx \prod_{m=1}^{M} \left\{ \frac{1}{N_z} \sum_{i=1}^{N_z} \frac{1}{N_w} \sum_{j=1}^{N_w} p(\mathbf{y}_{\tau^*}^m | \mathbf{x}_{\tau^*}^m, \mathbf{w}_{\tau^*,1:O}^{m}{}^{(j)}) \right\}, \tag{14}$$

where $\mathbf{w}_{\tau^*,1:O}^{m}{}^{(j)} \sim p_\phi(\mathbf{w}_{\tau^*,1:O}^{m} | \mathbf{z}_{\tau^*}^{m(i)}, \mathcal{C}_{\tau^*}^{1:M}; \omega)$ and $\mathbf{z}_{\tau^*}^{m(i)} \sim p_\theta(\mathbf{z}_{\tau^*}^m | \mathcal{C}_{\tau^*}^m; \nu^m)$. Here the Monte Carlo samples follow their corresponding prior distributions since the target sets are unavailable during the meta-test.

D More Experimental Details

D.1 Transformer-structured Inference Modules in Regression Scenarios

Here we present the implementation details of transformer-structured inference module θ in regression scenarios. In a single episode τ, the module θ encodes the task-specific information into each refined task-specific token ν^m, and then infers the prior distribution or the variational posterior distribution for the global latent representation $\mathbf{z}_\tau^m$. For episodic multi-task regression, the local latent parameters $\mathbf{w}_{\tau,1:O}^{m}$ construct a task-specific regressor during inference. We assume that the output of the decoder follows a Gaussian distribution for regression tasks. Thus, $\mathbf{w}_{\tau,1:O}^{m}$ are instantiated as parameters for generating the mean and variance of predictions.

D.2 Backbone and Training Details

Following the protocol of [10], we apply the pre-trained deep model as the backbone for the proposed method and baselines to extract the input features under the episodic multi-task classification setup. To be specific, we adopt VGGnet [106] for `Office-Home`, and its feature size is 4096. We take ResNet18 [107] for `DomainNet` with input size 512. In practice, we train our method and baselines by the Adam optimizer [108] using an NVIDIA Tesla V100 GPU. The learning rate is initially set as $1e-4$ and decreases with a factor of 0.5 every $3,000$ iterations.

E Algorithm of the proposed HNPs

F More Experimental Results under Episodic Multi-Task Setup

F.1 Effects of More "Tasks"

To investigate the effects of more "tasks" in the episodic multi-task setup, we perform experiments on Office-Home under the Xway5way1shot setup by gradually increasing tasks during inference. Table 11 shows that the average accuracy increases with more tasks. The main reason is that more tasks can provide richer transferable information. Our model benefits from the positive transfer among tasks, and thus obtaining higher performance gain from more tasks.

Algorithm 1: Meta-training phase of HNPs.

Input : M distinct and relevant task distributions $p(\mathcal{I}^{1:M})$, numbers of Monte Carlo samples N_z and N_w, learning rates α.

Output: Meta-trained transformer inference module θ and ϕ, learnable tokens $\omega_{1:O}$ and $\nu^{1:M}$.

Initialize transformer inference module $\{\theta, \nu^{1:M}\}$;
Initialize transformer inference module $\{\phi, \omega_{1:O}\}$;
while *Meta-Training not Completed* **do**

    // sample a meta-training episode indexed with τ.
    for $m = 1$ *to* M **do**
        Sample a task $\mathcal{I}_\tau^m \sim p(\mathcal{I}^m)$, which shares the same target space $\mathcal{Y}_\tau$ with other tasks in the episode;
        Sample a context set $\mathcal{C}_\tau^m$ and a target set $\mathcal{T}_\tau^m$ for the task $\mathcal{I}_\tau^m$;
    end
    // infer hierarchical latent variables.
    for $m = 1$ *to* M **do**
        Apply transformer inference module θ to infer prior and variational posterior distributions over $\mathbf{z}_\tau^m$ as Eq. (5), Eq. (6), and Eq. (7) in the main paper;
        Draw N_z samples from the variational posterior, $\{\mathbf{z}_\tau^{m(i)}\}_{i=1}^{N_z}$;
        for $i = 1$ *to* N_z **do**
            for $o = 1$ *to* O **do**
                Apply transformer inference module ϕ to infer prior and variational posterior distributions over $\mathbf{w}_{\tau,o}^m$ as Eq. (8), Eq. (9), and Eq. (10) in the main paper;
                Draw N_w samples from the variational posterior, $\{\mathbf{w}_{\tau,o}^{m\,(j)}\}_{j=1}^{N_w}$;
            end
        end
    end
    // optimize the objective.
    Compute predictive distributions and minimize the empirical objective in Eq. (13) ;
    Update θ, ϕ, $\omega_{1:O}$ and $\nu^{1:M}$ with learning rate α.
end

F.2   4task20way1shot v.s. 20way4shot

To show the effectiveness of the proposed method, we conduct experiments with the 20-way 4-shot setup, which needs to mix samples from all tasks in one episode. As shown in Table 12, MAML and Proto.Net perform better under the 20-way 4-shot but cannot outperform our method. The main reason is that our method can better handle distribution shifts among tasks by exploring task-relatedness rather than simply mixing them together.

F.3   Comparisons with More Recent Works

To compare the proposed method with more recent works, we perform experiments on Office-Home under the 4task5way1shot and 4task5way5shot setups. We provide some brief descriptions of two recent works as follows:

[76] theoretically addresses the conclusion that MTL methods are powerful and efficient alternatives to GBML for meta-learning applications. However, our method inherits the advantages of multi-task learning and meta-learning: simultaneously generalizing meta-knowledge from past to new episodes and exploiting task-relatedness across heterogeneous tasks in every single episode. Thus, our method is more suitable for solving the data-insufficiency problem.

[109] augments the task set in meta-learning through interpolation. Our method fully utilizes several observed tasks in a single episode rather than generating additional tasks.

Table 13 shows that our method significantly outperforms other baselines with severely insufficient data, such as 1-shot. This is consistent with the conclusion obtained in the main paper.

Algorithm 2: Meta-test phase of HNPs.

Input :Meta-trained transformer inference module θ and ϕ, learned tokens $\omega_{1:O}$ and $\nu^{1:M}$, numbers of Monte Carlo samples N_z and N_w.
Output :Prediction results.
while *Meta-Test not Completed* **do**
    // given a meta-test episode indexed with τ^*.
    Collect the context sets of all tasks in the episode, $\mathcal{C}_{\tau^*}^{1:M}$.
    for $m = 1$ *to* M **do**
        Apply transformer inference module θ to infer prior distributions over $\mathbf{z}_{\tau^*}^m$ as Eq. (5), Eq. (6), and Eq. (7) in the main paper;
        Draw N_z samples from the prior distribution, $\{\mathbf{z}_{\tau^*}^{m\,(i)}\}_{i=1}^{N_z}$;
        for $i = 1$ *to* N_z **do**
            for $o = 1$ *to* O **do**
                Apply transformer inference module ϕ to infer the prior distribution over $\mathbf{w}_{\tau^*,o}^m$ as Eq. (8), Eq. (9), and Eq. (10) in the main paper;
                Draw N_w samples from the prior distribution, $\{\mathbf{w}_{\tau^*,o}^{m\,(j)}\}_{j=1}^{N_w}$;
            end
        end
    end
    Perform predictions on the target sets in Eq. (14) ;
end

Table 11: **Performance comparisons on Office-Home under the Xtask5way1shot setup during inference.**

Number of tasks	1	2	3	4
Average accuracy	64.33 ± 0.85	70.75 ± 0.67	74.95 ± 0.57	76.29 ± 0.51

F.4 Comparisons on Another Benchmark Dataset

We validate the performance of methods on the Office31 dataset [110, 111] under the 3task5way1shot setup. This dataset contains 31 object categories in three domains: Amazon, DSLR, and Webcam. Table 14 shows our method outperforms baseline methods, demonstrating our model's effectiveness in addressing the data insufficiency under the episodic setup.

G More Experimental Results under Conventional Multi-Task Setup

To show comparisons with existing multi-task models, which are designed for conventional multi-task learning, we extend the proposed HNPs to conventional multi-task learning settings for both regression and classification tasks by considering only one episode during training and inference. Under conventional multi-task settings (MIMO), we investigate their effectiveness in exploring shared knowledge when limited tasks and samples are available during training.

G.1 Conventional Multi-Task Regression

Dataset and Settings. We show the effectiveness of HNPs for conventional multi-task regression. We design experiments for rotation angle estimation on the `Rotated MNIST` dataset [112]. Each task is an angle estimation problem for a digit, and different tasks corresponding to individual digits are related because they share the same rotation angle space. Each image is rotated by $0°$ through $90°$ in intervals of $10°$, where the rotation angle is the regression target. We randomly choose 0.1% training samples per task per angle as the training set.

We use the average of normalized mean squared errors (NMSE) of all tasks as the performance measurement. The lower NMSE, the better the performance. We provide 95% confidence intervals for the errors from five runs. Descriptions of baselines can be found in Section G.2.

Table 12: **Performance comparisons under the 4task20way1shot and 20way4shot setups.**

Methods	4task20way1shot	20way4shot
MAML	34.29 ± 0.19	37.23 ± 0.25
Proto.Net	32.72 ± 0.18	37.12 ± 0.22
Ours	51.82 ± 0.23	-

Table 13: **Performance comparisons with more recent baselines.**

Methods	1-shot	5-shot
MTL-bridge [76]	64.31 ± 0.55	75.10 ± 0.51
MLTI [109]	70.69 ± 0.73	79.59 ± 0.58
Ours	76.29 ± 0.51	80.80 ± 0.42

Results and Discussions. The experimental results are summarized in Table 15. The proposed HNPs outperform other counterpart methods by yielding a lower mean error. This demonstrates the effectiveness of HNPs in capturing task-relatedness for improved regression performance.

G.2 Conventional Multi-Task Classification

Datasets and Settings. `Office-Caltech` [113] contains ten categories shared between Office-31 [110] and Caltech-256 [114]. One task uses data from Caltech-256, and the other tasks use data from Office-31, whose images were collected from three distinct domains/tasks, namely Amazon, Webcam and DSLR. There are $8 \sim 151$ samples per category per task and $2,533$ images. `ImageCLEF` [10], the benchmark for the ImageCLEF domain adaptation challenge, contains 12 common categories shared by four public datasets/tasks: Caltech-256, ImageNet ILSVRC 2012, Pascal VOC 2012, and Bing. There are $2,400$ images in total. `Office-Home` [91] mentioned in the main paper is also used under this setting.

We adopt the standard evaluation protocols [10] for multi-task classification datasets. We randomly select 5%, 10% and 20% labeled data for training, which correspond to about 3, 6 and 12 samples per category per task, respectively. In this case, each task has insufficient training data for building a reliable classifier without overfitting. The average accuracy of all tasks is used for measuring the overall performance. We again provide 95% confidence intervals for the errors from five runs.

Alternatives Methods. We conduct a thorough comparison with alternative multi-task learning models. Single-task learning (STL) is implemented by task-specific feature extractors and predictors without knowledge sharing among tasks. Basic multi-task learning (BMTL) shares feature extractors and adds task-specific predictors. We also define variational extensions of single-task learning (VSTL) and basic multi-task learning (VBMTL), which treat predictors as latent variables [11]. For a fair comparison, all the baseline methods mentioned above share the same architecture of the feature extractor and the train-test splits. We also compare the proposed HNPs to representative multi-task models. MTL-Uncertainty [24], MRN [10], LearnToBranch [48] are deep MTL methods, employing deep neural networks to construct information-sharing mechanisms for tasks. TCGBML [35], MTVIB [41] and VMTL [11] are probabilistic MTL methods, applying Bayes frameworks to model the relationships among tasks.

Results and Discussions. We provide more comprehensive comparisons on `Office-Home`, `Office-Caltech` and `ImageCLEF` in Table 16. The best results are marked in bold. Our HNPs achieve competitive and even better performance on conventional multi-task classification datasets with different train-test splits. VSTL and VBMTL perform better than STL and BMTL, demonstrating the benefits of Bayes frameworks. Compared with multi-task probabilistic baselines, including VBMTL, TCGBML, MTVIB and VMTL, our HNPs can model more complex functional distributions with more powerful priors by inferring both representations and parameters for predictive functions.

Compared with VMTL [11], which neglects the hierarchical architecture of latent variables, the proposed HNPs show better performance. This demonstrates that by modeling the complex dependencies between heterogeneous context sets within the hierarchical Bayes framework, HNPs explore

Table 14: **Performance comparisons on the Office31 dataset.**

Methods	ERM	Proto.Net	CNPs	NPs	TNP-D	Ours
Average Accuracy	63.53 ± 0.71	64.54 ± 0.64	49.02 ± 0.74	40.52 ± 0.75	69.69 ± 0.87	71.89 ± 0.52

Table 15: **Conventional multi-task regression (normalized mean squared errors) for rotation angle estimation.**

Methods	Average NMSE
STL	$.215 \pm.001$
VSTL	$.224 \pm.004$
BMTL	$.118 \pm.003$
VBMTL	$.121 \pm.003$
LearnToBranch [48]	$.109 \pm.002$
VMTL [11]	$.110 \pm.003$
HNPs	$\mathbf{.103} \pm.001$

task-relatedness better. The hierarchical Bayes framework enables our model to explore the relevant knowledge even in the presence of distribution shifts among tasks.

H Application to Brain Image Segmentation

To show that HNPs have the potential to be helpful in settings other than categorization and regression, we apply the proposed HNPs to brain image segmentation.

Dataset and Settings. We adopt a brain image dataset [115] with lower-grade gliomas collected from 110 patients. The number of images varies among patients from 20 to 88. The goal is to segment the tumor in each brain image by predicting its contour.

We reformulate the segmentation task as a pixel-wise regression problem, where each pixel corresponds to a regression task to predict the probability of this pixel belonging to the tumor. In doing so, the spatial correlation and dependency among pixels are effectively modeled by capturing task-relatedness. For the task m, we define Ω_m as a local region centered at the spatial position m, which provides the local context information. In this case, the region centered at the pixel provides the local context information. Each task incorporates the knowledge provided by related tasks into the context of the predictive function. This offers an effective way to model the long-range interdependence of pixels in one image. In the implementation, we use U-Net [116] as the backbone and append our model to the last layer.

Results and Discussions. The proposed HNPs surpass the baseline U-Net by 0.8% (91.2% v.s. 90.6%) in terms of dice similarity coefficients (DSC) for the overall validation set. We provide the

Table 16: **Classification performance (average accuracy) on `Office-Home`, `Office-Caltech` and `ImageCLEF`.**

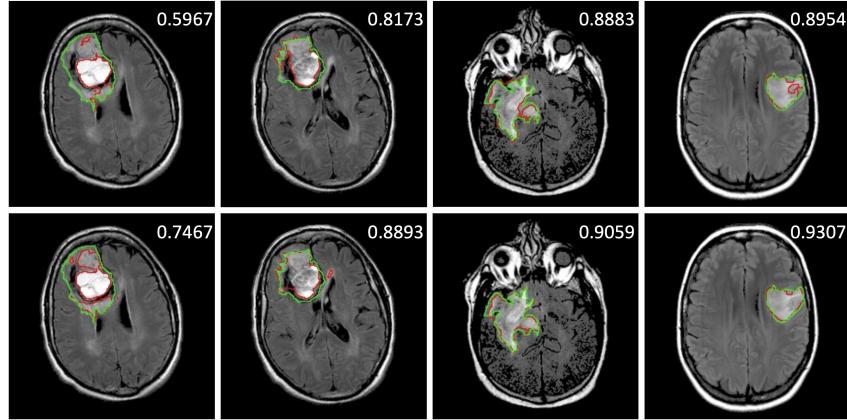| Methods	Office-Home			Office-Caltech			ImageCLEF		
	5%	10%	20%	5%	10%	20%	5%	10%	20%
STL	49.2 ± 0.2	58.3 ± 0.1	64.9 ± 0.1	88.6 ± 0.3	90.7 ± 0.2	92.4 ± 0.3	62.6 ± 0.2	69.7 ± 0.3	76.2 ± 0.3
VSTL	51.1 ± 0.1	60.2 ± 0.2	65.8 ± 0.2	89.0 ± 0.2	91.1 ± 0.2	93.4 ± 0.3	64.9 ± 0.3	70.8 ± 0.3	77.2 ± 0.2
BMTL	50.4 ± 0.1	59.5 ± 0.1	65.6 ± 0.1	89.5 ± 0.3	92.3 ± 0.2	93.1 ± 0.1	65.7 ± 0.4	72.0 ± 0.3	76.8 ± 0.3
VBMTL	51.3 ± 0.1	60.9 ± 0.1	67.0 ± 0.2	90.8 ± 0.6	93.2 ± 0.2	93.5 ± 0.1	67.1 ± 0.3	73.0 ± 0.7	78.0 ± 0.2
MTL-Uncertainty[24]	51.8 ± 0.1	57.2 ± 0.2	66.8 ± 0.2	91.2 ± 0.3	93.8 ± 0.2	94.7 ± 0.3	74.6 ± 0.2	76.9 ± 0.3	79.2 ± 0.3
MRN [10]	57.4 ± 0.1	63.4 ± 0.2	67.1 ± 0.1	93.4 ± 0.2	94.8 ± 0.3	95.1 ± 0.1	73.7 ± 0.4	75.8 ± 0.2	79.7 ± 0.3
LearnToBranch [48]	38.3 ± 0.5	51.5 ± 0.3	62.2 ± 0.4	74.6 ± 0.9	80.4 ± 1.2	89.9 ± 0.8	51.7 ± 0.9	62.6 ± 0.8	71.6 ± 0.4
TCGBML[35]	52.8 ± 0.1	60.0 ± 0.2	68.7 ± 0.2	91.8 ± 0.1	95.0 ± 0.2	95.1 ± 0.1	73.9 ± 0.3	76.5 ± 0.4	79.3 ± 0.4
MTVIB [41]	49.9 ± 0.2	55.3 ± 0.1	66.2 ± 0.1	91.1 ± 0.3	94.1 ± 0.3	95.0 ± 0.2	74.0 ± 0.4	77.3 ± 0.3	78.9 ± 0.5
VMTL [11]	58.3 ± 0.1	65.0 ± 0.0	69.2 ± 0.2	93.8 ± 0.1	95.3 ± 0.0	95.2 ± 0.1	76.2 ± 0.3	77.9 ± 0.2	80.2 ± 0.1
HNPs	$\mathbf{60.0} \pm 0.1$	$\mathbf{66.2} \pm 0.2$	$\mathbf{70.9} \pm 0.2$	$\mathbf{94.6} \pm 0.1$	$\mathbf{95.4} \pm 0.1$	$\mathbf{95.8} \pm 0.1$	$\mathbf{76.4} \pm 0.1$	$\mathbf{79.5} \pm 0.1$	$\mathbf{80.9} \pm 0.1$

Figure 7: **Segmentation results by HNPs (bottom row) and U-Net (upper row)**. The ground truth contours are in green, and the predicted ones are in red. The numbers are DSC scores computed against the ground truth. HNPs can predict contours closer to the ground truth ones, indicating the advantages of exploring spatial context information for image segmentation.

predicted contours by HNPs (bottom row) and the U-Net (upper row) in Figure 7, where the green outline corresponds to the ground truth and the red to the segmentation output. This figure shows that HNPs predict contours closer to the ground truth. The results demonstrate the advantages of HNPs in exploring spatial-relatedness for medical segmentation.